HEAT TRANSFER DURING FILM CONDENSATION OF POTASSIUM VAPOR

DETLEV GUSTAV KROGER

Engineering Projects Laboratory
Massachusetts Institute of
Technology

DSR Report No. 75239-42

Center for Space Research
NsG-496

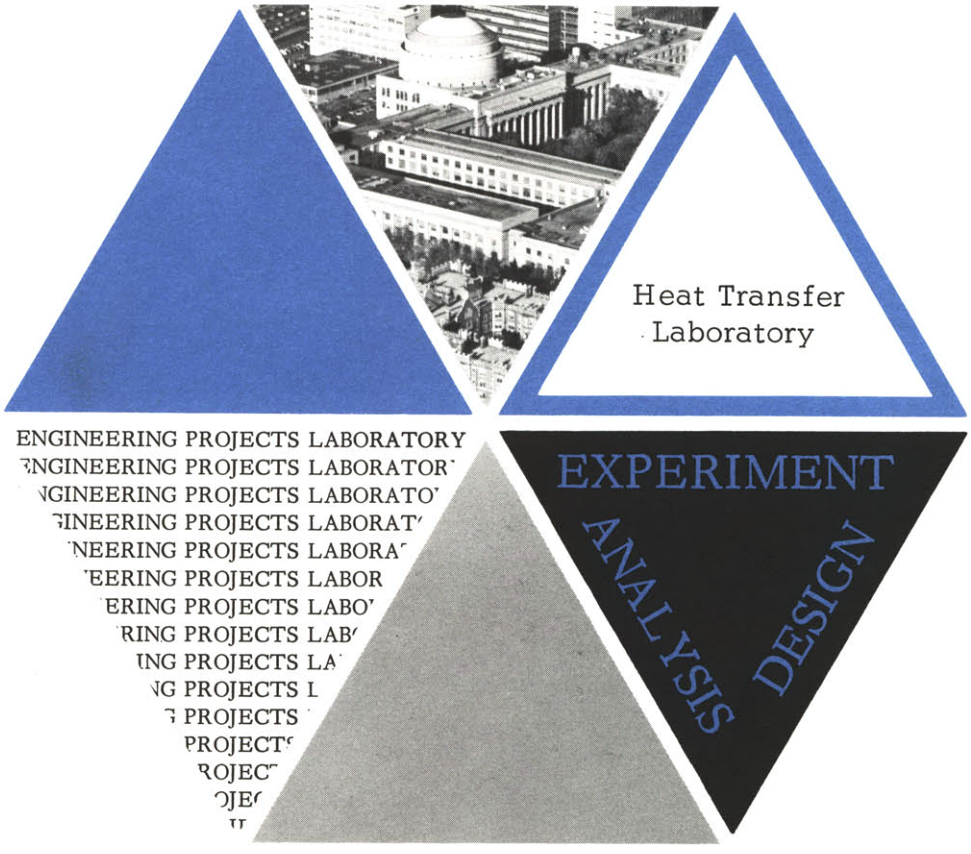

HEAT TRANSFER DURING FILM CONDENSATION OF POTASSIUM VAPOR

by

Detlev Gustav Kroger

Submitted to the Department of Mechanical Engineering on August 18, 1966, in partial fulfillment of the requirements for the degree of Doctor of Science.

ABSTRACT

The object of this work is to investigate theoretically and experimentally the following two phases of heat transfer during condensation of potassium vapor:

a. Heat transfer during film condensation of pure saturated potassium vapor on a vertical surface.

b. Heat transfer during film condensation of potassium vapor in the presence of a small quantity of non-condensable gas.

Investigators have until recently been unable to explain the large discrepancy between theory and experiment for the case of heat transfer during film condensation of pure liquid metal vapors. Calculations from kinetic theory and irreversible thermodynamics suggest that this difference may be due to a significant thermal resistance at the liquid-vapor interface in addition to that of the condensate film. This interfacial resistance becomes especially noticeable at low vapor pressures and is dependent on a "condensation" coefficient to be determined experimentally.

The presence of a trace of non-condensable gas during condensation may greatly reduce the heat transfer rate. An analysis predicting the heat transfer rate during condensation of potassium vapor in the presence of a non-condensable gas is presented, and experiments are performed to test the validity thereof.

Thesis Supervisor: Warren M. Rohsenow
Title: Professor of Mechanical Engineering

ACKNOWLEDGMENTS

The author wishes to express his sincerest thanks to Professor Warren M. Rohsenow, his Thesis Supervisor, for suggesting the topic and Professor Peter Griffith and Dr. George N. Hatsopoulos in their capacity as members of the thesis committee.

A word of thanks also to Professors Edwin J. Le Fevre, Walter J. Bornhorst, and Mr. Robert R. Adt for many valuable discussions and Miss Lucille Blake for typing this thesis.

This work was supported by the Center for Space Research under contract number NsG-496 and was done in part at the Computation Center at the Massachusetts Institute of Technology, Cambridge, Massachusetts.

TABLE OF CONTENTS

LIST OF FIGURES

NOMENCLATURE

A	area
A^*, B^*, C^*	functions of $\frac{KT}{\varepsilon}$
C	constant
c_p	specific heat
D_{ij}	binary diffusion coefficient
D_i^T	thermal diffusion coefficient
g	gravitational acceleration
h	enthalpy or heat transfer coefficient
h_{fg}	latent heat of vaporization
J_u	energy flux
j	mass flux with respect to mass average velocity
K	Boltzmann constant
k	thermal conductivity
k_T	thermal diffusion ratio
L	Avogadro's number
l	length
M	molecular weight
m	mass per molecule
n	number density
p	pressure per unit area
q_c	condensation heat flux
R	universal gas constant
T	temperature
T_b	boiling temperature
T_{Av}	average temperature

t	effective gas thickness
$\bar{V}$	diffusion velocity
$\bar{v}$	average molecular velocity
v_o	mass average velocity
v_b	mole volume
v_{fg}	difference between vapor and liquid specific volume
W	mass of non-condensable gas
w	mass flux
X_k	external forces
ε_o	emissivity
γ	ratio of specific heats
ε/K	potential energy parameter
Γ	correction factor as defined by equation (4)
μ	dynamic viscosity
$\Omega^{(22)*}$ $\Omega_{12}^{(11)*}$	collision integrals
ρ	density
σ	condensation coefficient or interaction parameter

Subscripts

i	interface
i, j	i-th and j-th components
l	liquid
m	vapor-gas mixture
s	condensate surface
v	vapor
w	wall

I. INTRODUCTION

In recent years liquid metals have found increasing use as heat transfer media in nuclear reactors in conventional power plants and also in space power generating units. The use of nuclear power incorporating liquid metals as working fluid offers an excellent source of power for space application. High temperature operation improving heat rejection by radiation in space, high thermal conductivity, and low vapor pressure resulting in lighter and more compact units are some of the advantages gained by using liquid metals.

The present work includes a theoretical and experimental investigation of heat transfer during condensation of potassium vapor and the effect of the presence of traces of non-condensable gases on the heat transfer coefficient. This latter effect is of significance in nuclear reactors, where cover gases such as helium or argon are used, and their presence in the system especially during a scram may impair removal of the afterglow energy.

I.1. Review of the Literature

The problem of condensation heat transfer was first formulated by Nusselt,[1] and his analysis was later modified and extended by other investigators. Seban[2] extended Nusselt's analysis for the case of higher Reynolds number. Bromley[3] included the effects of subcooling of the condensate, and Rohsenow[4] allowed for non-linearities in the film temperature distribution. Mabuchi[5] and Sparrow and Gregg[6] considered momentum changes in the condensate film. Chen,[7] Koh, Sparrow, and Hartnett,[8] Koh,[9] and Chato[10] considered the effect of vapor drag.

Although experiments have substantially borne out the theoretical predictions for liquids with $Pr > 0.5$,[11] the same cannot be said for liquid metals where experimental heat transfer rates were found to be five to thirty times smaller than predicted. References (12), (13), (14), (15), (16), and (17) are but a few indicating this trend. The discrepancy may be due to any of the following effects:

a. A resistance at the solid-liquid interface.

b. A film thickness other than that predicted by Nusselt's theory.

c. The presence of non-condensable gases.

d. Impurities on the condensate surface.

e. A resistance at the liquid-vapor interface.

The presence of a thermal resistance at the solid-liquid interface may be due to the formation of oxide layers, adsorbed gases, or chemical reactions between the condensate and the wall. By taking the necessary precautions, such as adequate outgassing of the system, correct choice of condensing plate material, and careful cleaning of the condensing surface, this resistance may be eliminated.

The condensate film thickness is not expected to deviate substantially from Nusselt's prediction. This expectation was verified by Sukhatme[15] who measured the film thickness during condensation of mercury vapor on a vertical cylindrical surface.

The presence of small traces of non-condensable gases in the system may severely reduce the condensation heat transfer rate. Continuous purging and an absolutely leak-tight system can eliminate this problem.

During condensation it is highly unlikely that any impurities occur at the condensate film surface.

The resistance at the liquid-vapor interface, which had until recently received very little attention, thus appears to be of considerable consequence during condensation of liquid metal vapors. The nature of this resistance and application of the modified Hertz-Knudsen equation for interphase mass transfer are discussed in some detail by Schrage.[18] Further reviews are presented by Wilhelm,[19] Mills,[20] and Barry.[21] A more rigorous solution to the problem of interphase mass transfer was recently presented by Bornhorst.[22] This thermodynamic approach to the problem is limited to relatively low mass transfer rates.

The presence of a non-condensable gas during condensation may considerably reduce the condensation heat transfer rate. Reynolds[23] first observed this effect in 1873. Othmer[24] showed that the heat transfer during condensation of steam may be reduced significantly due to the presence of a small amount of air. Similar tendencies were observed by Langen.[25] Experiments performed by Reed and Noyes[26] show the effect of non-condensables during condensation of sodium vapor. Sukhatme[15] showed qualitatively the strong influence of non-condensable gases during condensation of mercury.

Colburn[27],[28] and Chilton[29] analyzed this problem. Other investigators were Nusselt[30] and Merkel.[31] Various practical design procedures for condensers were proposed by Kern,[32] Bras,[33] and Cairns.[34] The most recent theory predicting condensation heat transfer in the presence of a non-condensable gas was derived by Sparrow.[35] The analysis is based on the conservation laws and appears to compare favourably with experimental results for air-steam mixtures.

II. ANALYTICAL CONSIDERATIONS

2.1 Heat Transfer during Film Condensation of a Saturated Vapor on a Vertical Surface

The object of this analysis is to predict the heat flux during film-wise condensation of saturated potassium vapor on a vertical surface, given the vapor and surface temperatures. It will be shown that an explicit solution for this problem is not possible unless a certain correction factor, to be found experimentally, is available. The present investigation includes the indirect determination of this factor employing the following analysis.

Consider a system as shown in Figure 1 where pure saturated potassium vapor at a known temperature T_v and a corresponding pressure p_v condenses film-wise on a clean vertical surface at a prescribed temperature T_w. It is assumed that the temperature distribution is as presented in Figure 1, where T_i is the vapor temperature at the liquid-vapor interface and T_s the condensate surface temperature.

Assuming the laminar condensate film to be adequately described by Nusselt's theory,[36] the condensation heat transfer rate is given by

$$q_c = 0.943 \sqrt[4]{\frac{g \rho (\rho_l - \rho_v) k^3 h_{fg}}{l \mu}} (T_s - T_w)^{3/4} \qquad (1)$$

where g, ρ_l, ρ_v, k, h_{fg}, l, and μ are respectively the gravitational acceleration, liquid density, vapor density, thermal conductivity of the liquid, latent heat of vaporization, length of condensing surface, and dynamic viscosity of the liquid. Minor refinements of this expression are possible, but may be neglected in this analysis.

Further expressions relating T_s and T_i at the liquid-vapor interface and T_i and T_v in the vapor are required to solve for q_c explicitly in terms of known values.

In a non-equilibrium liquid-vapor system, the interphase mass transfer rate is according to Schrage[18] given by

$$w = \left(\frac{M}{2\pi R}\right)^{1/2} \left(\frac{\sigma_s \, p_s}{T_s^{1/2}} - \frac{\Gamma \sigma_v \, p_v}{T_i^{1/2}}\right) \qquad (2)$$

where M is the molecular weight, R is the universal gas constant, and p_s is the saturation pressure corresponding to T_s. The correction factor Γ takes into consideration the effect of the vapor progress velocity.

The quantities σ_s and σ_v are variously known as "condensation" or "evaporation" coefficients. These factors may assume any value between zero and unity and allow for effects (in the case of monatomic molecules) such as interactions between condensing and evaporating molecules as well as any departures from the equilibrium Maxwellian velocity distribution in the vapor at the interface. It is obvious that at equilibrium conditions $\sigma_s = \sigma_v = \sigma$ where σ will be referred to as the "equilibrium condensation" coefficient or simply "condensation" coefficient. In this case σ, to be determined experimentally, may be a function of the thermodynamic state of the fluid and the type of molecule involved.

Restricting the analysis to cases that are only slightly non-equilibrium, i.e., $(T_i - T_s)/T_s \ll 1$ and $(p_v - p_s)/p_s \ll 1$, equation (2) may thus be written in simplified form as

$$w = \sigma \left(\frac{M}{2\pi R}\right)^{1/2} \left[\frac{p_s}{T_s^{1/2}} - \frac{\Gamma p_v}{T_i^{1/2}}\right] \qquad (3)$$

This simplification is not possible for highly non-equilibrium cases where σ_s and σ_v may depend on both the liquid and the vapor states as well as the type of molecule involved.

The correction factor Γ may be approximated by the following expression.(18)

$$\Gamma = 1 - \frac{w}{p_v\left(\frac{2M}{\pi RT_i}\right)^{1/2}} \tag{4}$$

Substitute this relation in (3) and find

$$w = \frac{2\sigma}{(2 - \sigma)} \left(\frac{M}{2\pi R}\right)^{1/2} \left(\frac{p_s}{T_s^{1/2}} - \frac{p_v}{T_i^{1/2}}\right) \tag{5}$$

The condensation heat flux is thus approximately

$$q_c = - wh_{fg} \tag{6}$$

A final relation between T_i and T_v is obtained by applying an energy balance to the vapor continuum (see Appendix E) giving

$$T_i - T_v = \frac{p_s v_{fg}}{2 c_p} + \frac{T_s(\gamma + 1)(2 - \sigma)}{2\gamma\sigma\left[0.5 - \frac{T_s(p_v - p_s)}{p_s(T_i - T_s)}\right]} \tag{7}$$

where v_{fg} is the difference between the vapor and the liquid specific volume, c_p is the specific heat, and γ the ratio of the specific heats.

The condensation heat flux q_c may be obtained by solving equations (1), (5), (6), and (7) simultaneously for a given value of σ.

It is noted that for most linear cases $T_s \approx T_i \approx T_v$, and equation (5) may be simplified to read

$$w = \frac{2\sigma}{(2 - \sigma)} \left(\frac{M}{2\pi RT_s}\right)^{1/2} (p_s - p_v) \tag{8}$$

and $$q_c = - \frac{2\sigma}{(2 - \sigma)} \left(\frac{M}{2\pi RT_s}\right)^{1/2} (p_s - p_v)\, h_{fg} \tag{9}$$

Kutcherov and Ricenglas[37],[38] obtained an equation similar to (8) for the interphase mass transfer. With this simplification introduced, q_c may be calculated directly from equations (1) and (9).

2.2 Heat Transfer during Film Condensation of Potassium Vapor on a Horizontal Surface in the Presence of a Small Quantity of Non-condensable Gas

The object of the following analysis is to predict the heat flux during condensation of potassium vapor containing a known amount of non-condensable gas. Consider a simple one-dimensional model as shown in Figure 2 in which saturated potassium vapor, continuously generated at (y = 1), diffuses through a non-condensable gas and condenses at the surface (y = 0). The latter surface may be regarded as being impervious to the gas, but not to the vapor.

According to Hirschfelder and Curtiss[39] the energy flux per unit area through a surface fixed with respect to the condensing surface in this case is given by

$$J_u = - k_m \frac{dT}{dy} + \sum_{i=1}^{\nu} h_i n_i m_i (\bar{V}_i + v_o) + \frac{KT}{n} \sum_{i=1}^{\nu} \sum_{\substack{j=1 \\ j \neq i}}^{\nu} \frac{n_j D_i^T}{m_i D_{ij}} (\bar{V}_i - \bar{V}_j) \tag{10}$$

where k_m is the thermal conductivity of the vapor-gas mixture (see Appendix A), h_i is the enthalpy per unit mass of the i-th component, K is the Boltzmann constant, n_i, n_j, and n are the number densities of the components and the mixture respectively, D_{ij} and D_i^T are the binary diffusion and thermal diffusion coefficients respectively (see Appendix A), v_o is the mass average velocity, m_i is the mass of the i-th particle, and $\bar{V}_i$ and $\bar{V}_j$ are the diffusion velocities of components i and j respectively.

In the present two-component system, let subscript 1 refer to the vapor and 2 to the gas. The diffusion velocity of the vapor may be expressed as

$$\bar{V}_1 = -\frac{n^2 m_2}{\rho n_1} D_{12} d_1 - \frac{D_1^T}{n_1 m_1 T} \frac{dT}{dy} = \bar{v}_1 - v_o \tag{11}$$

where ρ is the mass density and $\bar{v}_1$ is the average molecular velocity. The expression for d_1 includes concentration and pressure gradients as well as the effects of external forces X_k acting on the molecules.

$$d_1 = \frac{d}{dy}\left(\frac{n_1}{n}\right) + \left(\frac{n_1}{n} - \frac{n_1 m_1}{\rho}\right) \frac{d \ln p}{dy} - \frac{n_1 m_1}{p}\left[\frac{\rho}{m_1} X_1 - \sum_{k=1}^{\nu} n_k X_k\right]$$

In this case the only external force acting on the molecules is that of gravity, i.e.,

$$X_i = m_i g$$

Thus for a two-component system

$$\sum_{k=1}^{2} n_k X_k = (n_1 m_1 + n_2 m_2) g = \rho g$$

The external force term in the expression for d_1 thus vanishes

The gravitational acceleration, however, does lead to pressure diffusion. In the present system the variation in total pressure is less than 0.005%, and the second term containing $\frac{d}{dy}(\ln p)$ may be ignored.

Similarly the diffusion velocity of the gas is

$$\bar{V}_2 = \frac{n^2 m_1}{\rho n_2} D_{12} d_1 + \frac{D_1^T}{n_2 m_2 T} \frac{dT}{dy} = \bar{v}_2 - v_o \qquad (12)$$

since $D_{12} = D_{21}$ and $D_1^T = - D_2^T$ from considerations of mass conservation and because $\frac{n_1}{n} + \frac{n_2}{n} = 1$, thus $\frac{d}{dy}\left(\frac{n_1}{n}\right) = - \frac{d}{dy}\left(\frac{n_2}{n}\right)$.

Since the non-condensable gas is stagnant with respect to the fixed reference frame chosen, $\bar{v}_2 = 0$, and it follows from equation (12) that the mass average velocity is

$$v_o = - \left(\frac{n^2 m_1}{\rho n_2} D_{12} d_1 + \frac{D_1^T}{n_2 m_2 T} \frac{dT}{dy}\right) \qquad (13)$$

The mass flux of component 1 with respect to the mass average velocity v_o is

$$j_1 = n_1 m_1 \bar{V}_1 = \frac{n^2}{\rho} m_1 m_2 D_{12} d_2 - \frac{D_1^T}{T} \frac{dT}{dy}$$

A similar expression may be obtained for component 2. Taking the difference of these two expressions gives

$$\bar{V}_1 - \bar{V}_2 = - \frac{n^2}{n_1 n_2} D_{12} \left[\frac{d}{dy} \left(\frac{n_1}{n} \right) + \frac{k_T}{T} \frac{dT}{dy} \right] \tag{14}$$

where k_T, known as the thermal diffusion ratio is defined by,

$$k_T = \frac{\rho}{n^2 m_1 m_2} \frac{D_1^T}{D_{12}} \tag{15}$$

A theoretical first approximation to the thermal diffusion ratio k_T is presented in Appendix A.

According to expression(10), energy may be transported through a mixture by three mechanisms: (i) heat conduction; (ii) enthalpy flux; and (iii) a "reciprocal process" due to thermal diffusion.

During steady-state operation almost no gas will be found at the vapor generating surface, thus eliminating temperature and pressure gradients for all practical purposes. This means that the energy flux J_u across a fixed surface in this region will consist solely of the enthalpy flux of the vapor if the kinetic energy may be neglected. Furthermore, due to the conservation of energy, J_u remains constant throughout the system.

$$J_u = h_1 w \tag{16}$$

where h_1 is the enthalpy of the vapor, and w is the vapor mass flux per unit area at y = 1.

Substitute (11), (12), (13), (14), and (15) in (10), and find

$$J_u = - \left[k_m + \left(\frac{k_T}{T} \right) \alpha \right] \frac{dT}{dy} - \alpha \frac{d}{dy} \left(\frac{n_1}{n} \right) \tag{17}$$

where

$$\alpha = \frac{D_{12} n^2}{\rho} \left(h_1 m_1 m_2 + \frac{h_1 n_1 m_1^2}{n_2} + \frac{k_T p m_2}{n_1} \right)$$

and the total system pressure $p = nKT = p_1 + p_2$ is constant, consisting of the sum of the partial pressures p_1 and p_2 of the components.

According to the equation of state, the following relations exist:

$$n = \frac{pL}{RT}, \quad n_1 = \frac{p_1 L}{RT}, \quad n_2 = \frac{p_2 L}{RT}$$

where L is Avogadro's number, and R is the universal gas constant.

Further

$$m_1 = \frac{M_1}{L}, \quad m_2 = \frac{M_2}{L}$$

and $\rho = m_1 n_1 + m_2 n_2$

where M_1 and M_2 are the molecular weights of components 1 and 2, respectively.

Substitute these relations in (17) and find

$$J_u = - \left[k_m + \frac{\beta p k_T}{T} \right] \frac{dT}{dy} - \beta \frac{dp_1}{dy} \tag{18}$$

where

$$\beta = p D_{12} \left[\frac{h_1 M_1}{RT(p - p_1)} + \frac{p k_T M_2}{p_1 \left\{ p_1 M_1 + (p - p_1) M_2 \right\}} \right]$$

Another expression relating p_1 and T is obtained by applying the mass conservation equation to the vapor, i.e.,

$$m_1 n_1 \bar{v}_1 = m_1 n_1 \bar{V}_1 + m_1 n_1 v_o$$

or

$$w = m_1 n_1(\bar{V}_1 + v_o) \ . \tag{19}$$

Substitute (11) and (13) in (19), and find

$$w = - D_{12} \frac{m_1 n^2}{\rho} (m_2 + \frac{m_1 n_1}{n_2}) \frac{d}{dy} (\frac{n_1}{n}) - \frac{D_1^T}{T} (1 + \frac{m_1 n_1}{m_2 n_2}) \frac{dT}{dy}$$

This is further simplified by introducing k_T and applying the perfect gas relations

$$w = \frac{-D_{12} M_1 p}{RT(p - p_1)} \left[\frac{dp_1}{dy} + \frac{k_T p}{T} \frac{dT}{dy} \right] \tag{20}$$

Equations (18) and (20) are two simultaneous non-linear differential equations and can be solved numerically to give the temperature and partial pressure distributions in the system. The condensation heat transfer rate is

$$q_c = - w \left[h_{fg} + c_p(T_1 - T_o) \right] \tag{21}$$

where T_1 is the liquid temperature which corresponds to the vapor temperature at $y = 1$, T_o is the condensing surface temperature, h_{fg} is the latent heat of vaporization at T_1, and c_p is the specific heat of the liquid.

To find q_c the following procedure is proposed in cases where the film and interfacial resistance is negligible.

Given T_o and T_1 for the system containing a known amount of gas per unit condensing area, a first guess is made for w. Substitutew in (20)

and solve for the temperature distribution with boundary conditions T_o and T_1 and the pressure distribution with boundary conditions $p_1 = p$ at $(y = 1)$ and p_{10} the saturation pressure corresponding to T_o at $(y = 0)$. Knowing the temperature and partial pressure distribution of the gas makes it possible to calculate numerically, from the equation of state, the mass of gas in the system corresponding to the chosen value of w. If this gas mass does not agree with the known quantity in the system, a new value for w is chosen until agreement is obtained. The final choice of w is then substituted in (21) and q_c is found.

For engineering purposes a more approximate but adequate solution for finding the condensation heat transfer rate is suggested.

Usually for small quantities of gas $\frac{k_T p}{T} \frac{dT}{dp_1} \ll 1$, and the second term in equation (20) may be neglected resulting in

$$\frac{1}{(p - p_1)} \frac{dp_1}{dy} = \frac{- wRT}{D_{12} M_1 p} \tag{22}$$

From Appendix A, $D_{12} = C \frac{T^{3/2}}{p}$

Substitute this value in (22) and find

$$\frac{1}{(p - p_1)} \frac{dp_1}{dy} = \frac{- wR}{M_1 C T^{1/2}} \tag{23}$$

Since the pressure distribution is not significantly influenced by small variations in the absolute temperature, and since variations of the latter are relatively small when only a limited amount of gas is present, the assumption of an average constant temperature as a first approximation is more reasonable for calculating the partial pressure distribution in the system near the condensing surface.

Substitute $T_{Av} = \frac{(T_1 + T_o)}{2}$ in (23), and integrate assuming the pressure p_{10} at the condensing surface to be the saturation pressure of the vapor corresponding to the wall temperature. For all practical purposes the film and interfacial resistance may be neglected.

$$\frac{p - p_1}{p - p_{10}} = \exp\left(\frac{wR\,y}{M_1 C T_{Av}^{1/2}}\right)$$

The partial pressure distribution of the gas is thus

$$p_2 = p - p_1 = (p - p_{10}) \exp\left(\frac{wR\,y}{M_1 C T_{Av}^{1/2}}\right) \tag{24}$$

By integrating equation (24) over the total system height l, the mean partial pressure of the gas is obtained.

$$p_2{}^m = (p - p_{10}) \frac{M_1 C T_{Av}^{1/2}}{wRl} \left[\exp\left(\frac{wRl}{MCT_{Av}^{1/2}}\right) - 1 \right] \tag{25}$$

In the present experiments $\exp\left(\frac{wRl}{MCT_{Av}^{1/2}}\right) \ll 1$ and can be neglected. Thus

$$p_{2_m} = - (p - p_{10}) \frac{M_1 C T_{Av}^{1/2}}{wRl} \tag{26}$$

At this stage it is convenient to define an effective gas thickness. If all the non-condensable gas were to be concentrated in a pure layer adjacent to the condensing surface at the total system pressure and a temperature T_{Av}, this would be a measure of the amount of gas in the system.

The effective thickness expressed in terms of the mean partial pressure of the non-condensable gas is

$$t = \frac{lp_{2m}}{p} \tag{27}$$

Substitute (26) in (27) and find

$$w = -\frac{(p - p_{10})\, M_1 C T_{Av}^{1/2}}{p\, R\, t} \tag{28}$$

From (28) it follows that the condensation heat transfer rate per unit area is

$$q_c = -\frac{(p - p_{10})}{p}\ \frac{M_1 C T_{Av}^{1/2}}{t\, R}\ \left[h_{f_g} + c_p(T_1 - T_o)\right] \tag{29}$$

The condensation heat transfer coefficient is defined as

$$h_c = \frac{q_c}{(T_1 - T_o)} = \frac{(p - p_{10})}{p}\ \frac{M_1 C T_{Av}^{1/2}\left[h_{f_g} + c_p(T_1 - T_o)\right]}{t\, R\, (T_1 - T_o)} \tag{30}$$

where t is determined from the equation of state; i.e.,

$$t = \frac{WRT_{Av}}{AM_2 p}$$

with W the mass of noncondensable gas in the system, and A the condensing surface area.

III. DESCRIPTION OF THE EQUIPMENT

The liquid metal boiler condenser system was designed to investigate ultimately the following three cases of heat transfer during film condensation.

a. A pure saturated liquid metal vapor condensing on a vertical surface.

b. The effect of the presence of a small quantity of non-condensable gas during condensation.

c. A pure superheated liquid metal vapor condensing on a vertical surface.

A detailed description of the design considerations is presented in (40).

3.1 Summary of Apparatus

A detailed drawing presenting the major system components is shown in Figure 4 while Figure 3 shows the complete unit.

Low sodium grade potassium (25 lbs.) was supplied by the M. S. A. Company in a stainless steel container. The outlet of the latter is connected via a porous stainless steel filter to the boiler section of the system while the inlet is connected to the inert gas supply. Two narrow banded Watlow heaters of 3.75 KW output each are strapped to the reservoir.

The boiler is fitted with thirty-two radially located, sheathed Watlow Firerod heaters. A reducer is welded to the boiler, leading to a 13-in. long superheater section. Attached to the outside of this section is a resistance heater to compensate for heat losses to the environment. The superheater, which has been omitted in the present set of

experiments, consists essentially of an Alundum core in which a Kanthal Al resistance wire is embedded. The cylindrical core is housed between two concentric stainless steel cylinders. With a cylindrical core containing a condensate feedback pipe located on the inside of the superheater unit, there are thus two concentric annular openings through which the vapor may rise as shown.

The boiler and superheater sections are surrounded by a vacuum-tight outer stainless steel cylinder. This wall provides additional protection against possible liquid metal leakage. Furthermore, the space between the wall and the system, which contains Cerafelt 800 insulating material, can be filled with an inert gas. This prevents oxidation of the outer boiler and superheater surface during operation at high temperatures.

The upper end of the superheater section is fitted with a flange to which any condensing unit may be welded. In Figure 4 a unit containing a vertical condensing surface is shown in position. The surface is cooled on the outside by a constant temperature heat sink. In Figure 5 the vertical surface has been replaced by a unit containing a horizontal condensing surface. The heat sink has been relocated accordingly.

The heat sink which may contain boiling water or oil is connected to a water-cooled condenser the components of which are shown in Figure 6. The condensate is collected and weighed on a scale.

The condensing unit is connected via an air-cooled condenser, a cold trap, and a porous stainless steel filter to a mechanical vacuum pump.

Dried and purified inert gas, contained in the vertical gas reservoir may be added to the system whenever desired.

3.2 Major System Components

Although attempts were made to maintain maximum flexibility of the system, all joints in the boiler-condenser unit were heliarc welded to ensure an absolutely tight system. Whenever possible welds were so designed that they could readily beground away to make alterations possible.

Liquid Metal Boiler

The boiler section as shown in Figure 7 consists essentially of a 10-in. nominal (schedule 40) stainless steel 316 pipe which is heliarc welded to a 0.75-in. thick base plate. Thirty-two 0.84-in. o.d. holes for heating element sheaths are located in the pipe section. The sheaths are 4-in. long and have an inside diameter of 0.622 in. Watlow firerod cartridge heating units are inserted to supply an output of up to 18 KW. The large number of elements ensures flexibility over a wide range of heat input. To provide stable boiling,[41] nucleating sites are located on every heater sheath in the form of a porous weld. Three thermocouples are located in the boiler: one to indicate the liquid temperature and two in the vapor region. The boiler and superheater are shown in Figure 8 with the jacket lowered.

Condensing Surfaces

In the first phase of the experiment, saturated potassium vapor is condensed on a square vertical (4 in. X 4 in.) nickel 200 plate, 0.7-in. thick as pictured in Figure 9. Six, 0.063-in. diameter thermocouple holes are located in the plate. The complete condensing unit is shown

in Figure 10. An external resistance heater, clearly visible in Figure 10, facilitates removal of adsorbed gases prior to operation and compensates for some of the heat losses to the surroundings during the run. The entire unit is finally insulated with a layer of Cerafelt CRF-800 and enclosed in a vacuum-tight outer jacket that can be filled with an inert gas during operation to prevent oxidation of the unit at high temperatures.

During the second phase of the investigation, the vertical surface is replaced by a 4-in. diameter, 0.75-in. thick, horizontal, nickel 200 or stainless steel 316 disc pictured in Figure 11. Six 0.063 in. diameter thermocouple holes are located in the disc. The complete condensing unit with resistance heater is shown in Figure 12. The unit is insulated with a layer of Cerafelt CRF-800 and oxidation is prevented by a protective jacket of inert gas.

Non-condensable Gas Supply

A simple and accurate technique for measuring the quantity of gas to be added to the system is by means of the displacement method. Figure 14 shows the arrangement. With valve 2 closed, valve 1 is opened allowing the gas which has been dried by passing it through a molecular sieve bed containing pellets of alkali metal alumino-silicate maintained at liquid nitrogen temperature and purified through a Surfamax stainless steel filter with a mean pore size of five microns, to displace the mercury in the reservoir. With valve 1 closed, 2 is operated introducing the desired volume of gas into the system as indicated by the drop in mercury meniscus in the 50 cc buret.

Heat Sink

The constant temperature heat sink consists of a 10.75-in. o.d. stainless steel pipe, 18-in. high as shown in Figure 13. The sink is fitted with two copper surfaces. The horizontal piece is round having the same diameter as the nickel disc, while the vertical piece is the same size as the nickel plate. A central outlet allows the steam to escape to the condenser while a feedback pipe, used for short periods of time during warming up of the system and for refilling, extends to almost the bottom of the sink. A chromel-alumel thermocouple is installed to read the steam temperature. The entire sink is insulated with a 2-in. layer of Cerafelt CRF-800 which is held in position by an outer stainless steel jacket. The sink rests on three adjustable points for accurate vertical positioning. The supports rest in turn on phosphor-bronze surfaces such that they can move more easily in a horizontal direction. The horizontal adjustment is controlled by a crank.

3.3 Control and Measurement

The system control panel is shown in Figure 15. The three-phase mains supply 220 volts to a variable voltage transformer having a maximum output of 18 KW. This power is fed via six switches to the boiler heating elements. The current in each circuit is indicated by an ammeter for calculating the power supply. Separate variacs control the power output of the compensating resistance heaters attached to the condenser unit and the superheater section. The power supply to the liquid metal reservoir and the feed-line heating tapes is also independently controlled by variacs.

In case of overheating of the system, a thermostat located near the boiler activates a relay and all power is immediately shut off.

To detect possible "bumping" and the onset of stable boiling, a phonograph crystal is attached to one of the boiler supports. The vibrations are picked up by the cartridge and transmitted to an oscilloscope for observation.

The level of the liquid metal surface in the boiler is determined at any time by means of a gamma ray attenuation method. A radio-active source of Co-60 is mounted on a vertically adjustable support next to the boiler section. A scintillation counter (Model MRT 10-8) with a 1-in. diameter, 0.5-in. thick Thallium activated sodium iodide crystal affixed is located in line with the source on the opposite side of the boiler. The scintillation counter consists of a photomultiplier tube and a pre-amplifier. The photo tube is fed from a high voltage power supply (500 - 1360 V; Model 40-8B). The output of the pre-amplifier is fed into an amplifier discriminator (Model 30-19) before being counted on an electro-mechanical scalar (Model 40-30). The gamma ray generated by the source is picked up by the scintillation counter. When the level of the liquid metal rises such that it intercepts the ray, there is a sharp drop in the count rate.

All temperatures are measured by means of ungrounded chromel-alumel thermocouples the leads of which pass through an ice bath to multipole switches. The switches are connected to a precision potentiometer capable of reading to within 0.01 millivolt.

IV. EXPERIMENTAL PROCEDURE

Before making any runs, the system was carefully cleaned of oxides and greases. It was first exposed to a 50 per cent dilute solution of hydrochloric acid and thereafter flushed several times with distilled water. Trichloroethylene was then added as a degreaser. After flushing a few more times with distilled water, a reagent grade acetone was used as final rinse.

The system was then evacuated and outgassed at 700 ^{o}F for several hours. After checking for possible leaks in the system and feed pipes, the liquid metal in the reservoir was slowly heated to about 500 ^{o}F. The transfer lines, filter, and boiler were also kept at 500 ^{o}F. At this stage the reservoir was pressurized by means of an inert gas while the system was kept evacuated. On opening the supply valve the liquid metal was forced into the boiler section until it intercepted the gamma ray located at the desired operating depth. About 17 pounds of potassium were transferred. The system was then allowed to cool down and filled with helium at 15 psia.

Prior to each run the system was evacuated and then slowly heated to about 1100 ^{o}F without boiling taking place. At this stage the cooling water supply to the steam condenser was commenced, and the heat sink was brought into contact with the vertical condenser surface via a thermal resistance depending on the desired heat flux. These resistances consisted of various thicknesses of stainless steel. By increasing the power input the potassium was then brought to boil, and the temperature in the boiler was gradually raised to 1400 ^{o}F. The transition to stable

boiling (bumping) was clearly indicated on the oscilloscope in the form of intermittent sharp peaks, while stable boiling presented only small continuous fluctuations. After a few hours the water in the heat sink began to boil, and a quasi-steady state was attained by the system.

Throughout the heating period the temperature of the liquid, vapor, system wall, condensing wall, and cooling water was continually monitored.

Once steady state had been attained, the steam condensate weighing scale reading was noted. This reading was repeated every ten minutes during a run.

The vapor temperature T_v was found by reading two thermocouples in the vapor near the vertical condensing surface and averaging these values.

To find the wall temperature T_w, six thermocouples in the condensing plate were read. Furthermore, two thermocouples in the side walls of the condensing unit cylinder 0.25 in. and 0.75 in. from the condensing surface and two in the upper surface plate of the unit 0.25 in. and 0.5 in. from the surface were recorded. These temperature readings made it possible to determine the heat exchange between the nickel condensing plate and the system. The liquid temperature was also read.

After repeating the above set of readings every ten minutes for about one hour and obtaining consistent readings, the power input was reduced, and another set of readings was obtained after a steady state had been reached.

Although the system is vacuum tight, a little purging was done during operation.

With the horizontal condensing surface in position, a similar procedure was followed. The temperature readings included the six

thermocouples in the condensing plate, three thermocouples in the vapor, 1/4 in., 1/2 in., and 1 in. from the condensing surface, respectively, and the liquid temperature. Two thermocouples were also located immediately above the liquid surface and usually indicated the same temperature as the one in the liquid. Two thermocouples were located in the condensing unit wall 0.25 in. and 0.625 in. from the condensing surface from which the heat exchange by conduction between system and disc could be determined.

The first run was made without any gas present in the system. Thereafter the purge line was closed, and a known amount of gas was added to the system. After steady state had been reached, the thermocouples were again read every ten minutes, and the amount of steam condensate was noted.

After the first five tests the original horizontal condensing unit had to be replaced because of a fracture in one of the welds. The new unit differed from the original only in the sense that it was fitted with a 4-in. diameter stainless steel disc and did not have the reducer-type shape but was of uniform diameter.

V. EXPERIMENTAL RESULTS

5.1. Condensation of Saturated Potassium Vapor on a Vertical Surface

To determine the condensation coefficient σ from equations (1) and (9), the parameters T_v q_c, and T_w must be known.

The vapor temperature T_v was measured directly by means of two thermocouples located in the vapor near the condensing surface. The average value of these readings was noted. The corresponding saturation pressure p_v was calculated from an expression presented by Lemmon, et al.[42]

$$\log_{10} p = 4.185 - \frac{7797.6}{T} \tag{31}$$

where p is in atmospheres and T in degrees Rankine.

The condensation heat flux q_{cexp} was determined by two independent methods which proved to be quite consistent.

a. Two sets of three thermocouples each were so arranged in the condensing plate that two independent measurements of the temperature gradient in the wall were possible. With the resultant average gradient and a knowledge of the thermal conductivity of nickel 200,[43],[44] q_{cexp} was readily calculated.

b. The steam generated in the heat sink was condensed, collected, and weighed. Knowing the latent heat of vaporization of water at atmospheric pressure, q_{cexp} could be calculated.

As mentioned, thermocouples were located in the system walls to detect any heat leakage between the condensing surface and the system.

The amount of heat lost or gained by the plate in this way proved to be negligible.

The wall temperature T_w was found by extrapolating the temperature gradients obtained from the two sets of thermocouples located in the plate. In most cases the results agreed to within 1/2 ^{o}F.

With q_{cexp} and T_w known, T_s was calculated employing equation (1). The physical properties for potassium were taken from Weatherford[45] and evaluated at the wall temperature. The saturation pressure p_s corresponding to T_s was calculated using equation (31).

The vapor temperature T_i could be found from equation (7), but since in most cases $T_s \approx T_i \approx T_v$, equation (9) proved to be adequate for determining σ.

The effect of dimerization was neglected. The magnitude of the dimeric composition of potassium vapor is presented in Figure 19. In the present series of experiments, the mole fraction of dimer to vapor never exceeded 0.055.

In the tests performed the vapor pressure was varied from about 0.01 to 0.6 atmospheres, and the heat flux ranged between 34,000 and 99,000 Btu/hr.ft ^{2} as shown in Appendix B.

Figure (16) is a representation of the condensation coefficient as a function of the thermodynamic state of the condensate surface. At the higher pressure the scatter is somewhat more pronounced. This is probably due to the fact that a very small error in the wall or vapor temperature reading may result in a significant error in the corresponding pressure calculation, resulting in a similar deviation for σ. A

straight line correlating the data in the pressure range $0.004 < p_s < 1.0$ atmospheres is given by the following empirical equation

$$\sigma_{emp} = \frac{0.062}{p_s^{1/2}}$$

where p_s is in atmospheres.

5.2 The Effect of the Presence of a Non-condensable Gas on the Heat Transfer Rate during Condensation of Potassium Vapor

To predict the condensation heat transfer rate of potassium vapor in the presence of a non-condensable gas in our system, the liquid temperature T_l, the condensing surface temperature T_o, the total pressure p, and the type and quantity of gas must be specified.

The liquid temperature T_l, which should correspond to the vapor temperature immediately above the potassium surface during stable boiling because of the absence of any gas, was measured by means of one thermocouple in the liquid and two in the vapor near the surface. The readings of all three thermocouples were essentially the same.

Since all the non-condensable gas is concentrated in the vicinity of the condensing surface, it can be assumed that the total pressure p is the saturation pressure corresponding to T_l. Accordingly p was calculated employing equation (31).

The wall temperature was again calculated by extrapolating the temperature gradients obtained by two sets of three thermocouples located radially at different radii in the condensing disc. This method proved to be successful in the case where no gas or only a trace was present. With relatively large quantities of gas present, however, there was a

considerable temperature drop in the vapor towards the condensing surface and a resultant similar gradient in the system wall. Figure (17) shows the measured system wall temperature distribution for two typical cases containing different quantities of gas. The experimentally measured vapor temperature distribution is also shown. It should be noted that these temperature measurements in the vapor are approximate indications of the local vapor saturation temperature. The theoretically calculated vapor pressure distribution is also shown.

Because of the large temperature gradients in the system wall towards the condensing surface, there was a considerable heat flux from the system to the disc resulting in a noticeable radial temperature distortion in the latter. Under these conditions the diffusion flow field was obviously not truly one-dimensional any longer excepting near the center as shown in Figure 18. For these cases the temperature gradient given by the set of thermocouples near the center of the disc was used to determine the wall temperature. In this region there was no significant temperature distortion, and the problem remained one-dimensional.

The volume of gas added to the system was measured as described previously. The gas pressure and temperature was also noted prior to introduction such that the mass added could be calculated from the equation of state.

The heat flux q_{cexp} was calculated from the temperature gradient indicated by the set of thermocouples located near the center of the disc.

The experimental data and results for a potassium-helium mixture are presented in Appendix C.

The radiation heat flux between the condensing surface and the system was subtracted from the measured heat flux $q_{c\ exp}$ to obtain q_c. Assuming the vapor to be at the temperature of the liquid surface T_1 and assuming the liquid condensate running down the side walls is also at this temperature, the radiation heat flux is

$$q_r = 0.1713 \times 10^{-8}\ \varepsilon_o\ (T_1^4 - T_o^4)$$

where ε_o may be obtained from the data presented by Frehafer (50) which was verified theoretically by Mott and Jones (51). It was assumed that ε_o is directly proportional to the absolute temperature with a value of 0.06 at 520 deg R.

The experimental condensation heat transfer coefficient is thus expressed as

$$h_{c\ exp} = \frac{(q_{c\ exp} - q_r)}{(T_1 - T_o)}$$

The value $q_{c\ exact}$ representing the condensation heat flux was obtained by solving the two differential equations (18) and (20) numerically on a digital computer, while $q_{c\ approx}$ was obtained by employing equation (29). The usefulness of the approximate solution becomes obvious when it is noted that the maximum deviation from the exact solution is only 5.9 per cent in the case of helium. The reason for this insignificant deviation is ascribable to the fact that $\frac{k_T p}{T}\left(\frac{dT}{dp_1}\right) \ll 1$ and because the final result is only a weak function of temperature, suggesting that the use of an average temperature T_{Av} is adequate. The local magnitudes of $\frac{k_T p}{T}\left(\frac{dT}{dp_1}\right)$ for the various potassium-helium tests are shown in Figure 20. The maximum value attained was 0.05 during test number 6.

Good agreement was obtained between theory and experiment for the condensation heat transfer coefficient in the case of helium as is shown in Figure 21.

Test 11 was run with no gas present in the system. The analysis presented in 2.1 was applied to the data and the condensation coefficient was determined. Although Nusselt's theory is not applicable in this case, the temperature drop across the film is small compared to the interfacial difference, such that knowledge of the exact film thickness is of little consequence. The resultant value of σ is shown circled in Figure 16 and suggests that the system was free of all gases.

A more illustrative presentation of the significance of the presence of helium on the heat transfer coefficient during condensation is shown in Figure 22. This plot is for T_l = 1300 ^{o}F with the wall temperature ranging from 600 ^{o}F to 1200 ^{o}F, thus covering most of the experimental points except for tests 1, 5, and 6.

The experimental data and results for a potassium-argon mixture are presented in Appendix D. The nomenclature is the same as for the potassium-helium case. Two values for the wall temperature are given, i.e., $T_{o\ min.}$ and $T_{o\ max.}$.

During these experiments a quasi-steady operating state was never attained. Although the liquid temperature T_l and the amount of gas in the system was maintained constant for a specific test, the condensing wall temperature tended to fluctuate significantly throughout the test. For each test the maximum and minimum wall temperature was thus noted over a period of one hour or longer. All calculations were based on the minimum wall temperature reading.

A plot of the experimental heat transfer coefficient versus the theoretical heat transfer coefficient is shown in Figure 23. The discrepancy between theory and experiment is significant. In all cases the experimental heat transfer coefficient is considerably larger than the theoretical value, improving slightly for larger values of h_c, i.e., usually for tests having smaller quantities of argon present.

This discrepancy may be ascribed to the following:

a. Consider the present system in which potassium condenses in the presence of argon. Figure 24 illustrates such a case, showing the potassium flow lines and the lines of constant argon concentration. Although the conduction path between the system walls and the condensing plate was made as thin as possible, quantities of potassium condense on the walls which conduct away the resultant heat flux into the disc. This results in a distribution of argon over an area, larger than considered in the calculations, resulting in a smaller effective thickness at the center line where a greater heat flux may thus be expected.

b. Because of the diffusion of potassium towards the system wall, as described in a, there will be a resultant temperature gradient in that direction. Since argon has almost the same molecular weight as potassium, the density near the walls will be greater than at the center giving rise to convective currents as envisioned in Figure 25. This convective pattern is further encouraged by the condensate film on the walls and the fact that the diffusion coefficient

for potassium-argon is low. A further considerable decrease in the effective thickness may thus be expected. In addition pure potassium vapor is carried towards the condensing surface in the core of the convective current. Both these effects tend to increase the heat flux.

c. As was mentioned the temperature at the center of the disc fluctuated continuously. In a typical test the rate of fluctuation was noted. The temperature slowly fell from $T_{o\ max.}$ to $T_{o\ min.}$ in about three minutes. After remaining at $T_{o\ min.}$ for a few seconds, it suddenly rose to $T_{o\ max.}$ in a period of about eighteen seconds. After about thirty seconds, it again began to fall. Although not all fluctuations in any one test were identical, the times for the different phases were of the same order.

This phenomenon is explained in the following manner. The slow fall in T_o is due to the accumulation of argon at the condensing surface as a result of diffusion and convection. This results in a corresponding density rise at the condensing surface until the unstable situation so created is disturbed and the argon is suddenly removed, clearing the surface and exposing it to purer and hotter vapor. This immediately results in a larger heat flux, tending to rapidly raise the wall temperature after which the cycle is repeated. It is clear that this mechanism may result in a considerable increase in the average condensation heat transfer rate.

The significant effect of the presence of argon on the heat transfer coefficient is shown in Figure 26.

VI. DISCUSSION

A brief discussion of the application and validity of the analysis presented in section 2 is in order prior to a discussion of the experimental results.

6.1 Condensation of Saturated Potassium Vapor on a Vertical Surface

In the analysis prescribed in section 2.1, it was assumed that the thermal resistance at the liquid-wall interface was negligible. This assumption appears to be reasonable if one considers the fact that the theoretically predicted heat transfer rates are in close agreement with the experimental values for the flow of alkali metals in tubes as shown by Schroch[46] and Kirillov, et al.[49] After the first phase of experiments had been completed, the condensing surface was inspected, and although the surface had lost its original finish, it appeared to be free of impurities that may have resulted in an additional thermal resistance. The application of Nusselt's theory across the condensate film, which was quite laminar for all experimental runs, is in order. Furthermore, it is noted from the experimental results that the temperature drop across the film, assuming the above-mentioned theory to be valid, is almost an order of magnitude smaller than the interfacial drop. This suggests that minor refinements to Nusselt's theory may be ignored, and the use of an average heat transfer coefficient is permissible.

The problem of interphase mass transfer has received considerable attention recently. The most frequently and very often incorrectly applied expression for this phenomenon is the so-called modified Hertz-Knudsen equation which is discussed in some detail by Schrage.[8] This analysis

lacks rigor, in the sense that a simplified molecular model is assumed, and it is also incomplete since the energy and momentum conservation equations have not been considered.

Recently Bornhorst[22] presented a more rigorous solution to the problem by employing irreversible thermodynamics. He showed that the interphase mass transfer is given by

$$w = p_s v_{fg} \frac{L_{ii}}{T_s} \left[\left(\frac{K_b}{K_b + 1} \right) \frac{h_{fg}}{p_s v_{fg}} \left(\frac{\Delta T}{T_s} \right) - \frac{\Delta p}{p_s} \right] \tag{32}$$

where K_b and L_{ii} are unknown thermodynamic properties of the fluid, and $\Delta T = T_i - T_s$ and $\Delta p = p_v - p_s$ in the present model. It is readily shown that equation (5) can be written in the following manner:

$$w = \frac{2\sigma}{(2 - \sigma)} \left(\frac{M}{2\pi RT_i} \right)^{1/2} p_s \left(\frac{\Delta T}{2 T_s} - \frac{\Delta p}{p_s} \right) \tag{33}$$

This equation is similar to (32) in the sense that the "driving forces" appear in the same form. A comparison of equation (32) and (33) results in the following expression for σ.

$$\sigma = \frac{2 L_{ii}}{L_{ii} + \frac{2T_s}{v_{fg}} \left(\frac{M}{2\pi T_i R} \right)^{1/2}}$$

Since L_{ii} is a thermodynamic property of the fluid, the same must be true for σ.

Figure 27 presents the values for σ obtained by a number of different investigators for different alkali metals as a function of the state

of the fluid. The usefulness of the empirical expression for σ is clearly greatly enhanced by the fact that it correlates the data for various liquid metals. Most of the experimental results obtained by Sukhatme[15] and by Misra and Bonilla[12] were for highly non-equilibrium cases. Only their more linear tests were retained in Figure 27.

Because of the high heat fluxes required to maintain stable boiling at low vapor pressures, the present investigation was limited to a minimum pressure of about 0.01 atmosphere. The condensation coefficient tends to increase with decreasing pressure and eventually becomes unity as is shown by the data of Subbotin, et al.[17]

6.2 Condensation of Potassium Vapor in the Presence of a Non-condensable Gas

From the experimental results it is clear that the presence of a small amount of gas can greatly reduce the condensation heat transfer coefficient. The diffusion analysis presented in section 2.2 appears to be adequate in the absence of convective currents as was shown in the case of potassium condensing in the presence of helium on the lower side of a horizontal surface.

The significance of convective currents during condensation in the presence of a gas is clearly shown in the case of potassium condensing in the presence of argon on the lower surface of a horizontal disc. For design purposes the geometry of the system as well as the type of gas involved thus becomes of importance.

VII. RECOMMENDATIONS AND CONCLUSIONS

From the results obtained it is concluded that the most useful expression for design purposes for the case of condensation heat transfer across a vapor-liquid interface is given by equation (9). The empirical expression for the condensation coefficient may be used for monatomic liquid metals in the pressure range 0.004 to 1.0 atmospheres and may be assumed to be unity at lower pressures.

In the present analyses for interphase mass transfer, only linear cases have been considered. Further theoretical and experimental work for non-linear cases would be of value.

An experimental investigation of the transport coefficients appearing in Bornhorst's analysis is presently being conducted at the Massachusetts Institute of Technology.

When non-condensable gases are present in a condensing system, the proposed expressions for the condensation heat transfer rate are adequate depending on the geometry of the system in the absence of convective currents.

Additional experiments should be performed in which heavier alkali metals, e.g., mercury, condense in the presence of argon to test for the usefulness of the diffusion theory. If lighter vapors are to be condensed, condensation should take place on a horizontal surface facing upwards to minimize effects due to convection.

It has been suspected for some time that electrical surface charges may play a significant role during condensation heat transfer. A basic study of this phenomenon may prove to be of considerable value.

REFERENCES

1. Nusselt, W., Zeitsch. d. Ver. deutsch. Ing., 60, 541, (1916).
2. Seban, R. A., Trans. ASME, 76, 299, (1954).
3. Bromley, L. A., Ind. and Eng. Chem., 44, 2966, (1952).
4. Rohsenow, W. M., Trans. ASME, 78, 1645, (1956).
5. Mabuchi, I., Trans. Japan Soc. Mech. Engrs., 26, 1134, (1960).
6. Sparrow, E. M. and Gregg, J. L., Trans. ASME, Series C, 81, 13, (1959).
7. Chen, M. M., Trans. ASME, Series C, 83, 48, (1961).
8. Koh, C. Y., Sparrow, E. M., and Hartnett, J. P., Int. J. Heat and Mass Transfer, 2, 79, (1961).
9. Koh, C. Y., Trans. ASME, Series C, 83, 359, (1961).
10. Chato, J. C., ASHRAE Journal, 4 (2), 52, (1962).
11. McAdams, W. H., "Heat Transmission," McGraw-Hill, (1954).
12. Misra, B. and Bonilla, C. F., Chem. Eng. Prog. Sym., Series 18, 52, 7, (1956).
13. Cohn, P. D., M. S. Thesis, Oregon State College, (1960).
14. Roth, J. A., Report ASD-TDR-62-738, Wright-Patterson AFB, (1962).
15. Sukhatme, S. P., Ph.D. Thesis, M.I.T., (1964).
16. General Electric Co., Qtr. Report 9, Ctr. NAS 3-2528, Oct. 1964.
17. Subbotin, V. I., Ivanovsky, M. N., Sorokin, V. P., and Chulkov, V. A., Teplofizika vysokih temperatur, No. 4, (1964).
18. Schrage, R. W., "A Theoretical Study of Interphase Mass Transfer," Columbia University Press, New York, (1953).
19. Wilhelm, D. J., Ph.D. Thesis, Ohio State University, (1964).
20. Mills, A. F., Techn. Rep. NSF GP-2520, Series 6, 39, (1965).

21. Barry, R. E., Ph.D. Thesis, University of Michigan, (1965).

22. Bornhorst, W. J., Ph.D. Thesis, M.I.T., (1966).

23. Reynolds, O., Proc. Roy. Soc., 144, (1873).

24. Othmer, D. F., Ind. Eng. Chem., 21, (1929).

25. Langen, E., Forschung a.d. Geb. d. Ingenieurwes. 2, 359, (1931).

26. Reed, G. I., and Noyes, R. C., AEC Research and Development Report, NAA-SR-7325.

27. Colburn, A. P., Trans. AIChE, 29, 174, (1933).

28. Colburn, A. P., and Hougen, O. A., Ind. Eng. Chem. 26, 1178 (1934).

29. Chilton, T. H., and Colburn, A. P., Ind. Eng. Chem., 26, 1183, (1934).

30. Nusselt, W. A., angew. Math. Mech., 10, (1930).

31. Merkel, F. Z., Ver. dtsch. Ing., 72 (10), 342 (abstract), (1928).

32. Kern, D. Q., "Process Heat Transfer," McGraw-Hill Co., New York, (1950).

33. Bras. G. H., Chem. Engng. 60 (4), (5), (1953).

34. Cairns, R. C., Chem. Engng. Sci., 3 (1954).

35. Sparrow, E. M., and Lin, S. H., J. Heat and Mass Transfer, Series C, 86, 3, (1964)

36. Rohsenow, W. M., and Choi, H. Y., "Heat, Mass and Momentum Transfer," Prentice-Hall, Inc., (1961).

37. Kutcherov, R. Y. and Ricenglas, L. E., Journal of Experimental and Theoretical Physics, v. 37, issue 1(7), (1959).

38. Kutcherov, R. Y., and Ricenglas, L. E., Reports of AN SSSR 133, No. 5, (1960).

39. Hirschfelder, J. O., and Curtiss, C. F., "Molecular Theory of Gases and Liquids," John Wiley & Sons, Inc., New York, (1954).

40. Kroger, D. G., Mech. E. Thesis, M.I.T., (1965).

41. Marto, P. J., Ph.D. Thesis, M.I.T., 1965.

42. Lemmon, A. W., Deem, H. W., Hall, E. H., and Walling, J. P., "The Thermodynamic and Transport Properties of Potassium," Battelle Memorial Institute.

43. Hogan, C. L., and Sawyer, R. B., Jl. of Applied Physics, 23, 177, (1952).

44. The International Nickel Co., Inc., Technical Bulletin T-15.

45. Weatherford, W. D., Tyler, J. C., and Ku, P. M., "Properties of Inorganic Energy Conversion and Heat Transfer Fluids for Space Applications," Wadd Technical Report 61-96, (1961).

46. Schroch, S. L., Ph.D. Thesis, Purdue University, (1964).

47. Aladyev, I. T., et al., "Thermal Resistance of Phase Transition with Condensation of Potassium Vapor," Proceedings of the Third International Heat Transfer Conference, (1966).

48. Labuntsov, D. A., and Smirnov, S. I., "Heat Transfer in Condensation of Liquid Metal Vapors," Proceedings of the Third International Heat Transfer Conference, (1966).

49. Kirillov, P. L., Subbotin, V. I., Suvarov, N. Ya., Troyanov, M. F., Soviet Journ. Atomic Energy, 6, 253-60, (1960).

50. Frehafer, M. K., Phys. Rev. 15 (1920) 110.

51. Mott, N. F., and Jones, H., "The Theory of the Properties of Metals and Alloys, Oxford University Press, 1936.

APPENDIX A

Expressions for the Diffusion Coefficient, the Thermal Conductivity of a Binary Mixture, and the Thermal Diffusion Ratio

The following transport coefficients are obtained from Hirschfelder and Curtiss.[39]

The Diffusion Coefficient of a Binary Mixture

According to kinetic theory the binary diffusion coefficient may be expressed as

$$D_{12} = 0.002628 \frac{\sqrt{T^3 (M_1 + M_2)/2M_1M_2}}{p\sigma_{12}^2 \Omega_{12}^{(1,1)*}} \qquad \text{(A-1)}$$

where D_{12} = diffusion coefficient in cm^2/sec

p = pressure in atmospheres

T = temperature in ^oK

M_1, M_2 = molecular weights of species 1 and 2

σ_{12}, $\frac{\varepsilon_{12}}{K}$ = molecular potential energy parameters characteristic of interaction in A^o and ^oK, respectively

$\Omega_{12}^{(1,1)*}$ = collision integral

K = Boltzmann constant

Values of ε/K are obtained in the case of argon and helium from Hirschfelder and Curtiss,[39] while for potassium the potential parameter is calculated from the approximate relation

$$\frac{\varepsilon}{K} = 1.15\, T_b$$

where T_b is the boiling temperature in ^oK.

According to Hirschfelder and Curtiss[39] the value of KT/ε for a binary mixture is found from an empirical relation

$$\frac{KT}{\varepsilon_{12}} = \frac{KT}{\sqrt{\varepsilon_1 \varepsilon_2}}$$

The values of σ are tabulated in reference (39) for helium and argon. For potassium this parameter is obtained from the empirical relation

$$\sigma = 1.167\ v_b^{1/3} \quad (A^o)$$

where v_b = mole volume (cc/mole) at temperature T_b.

The mean collision diameter, according to Hirschfelder and Curtiss,[39] may be expressed as

$$\sigma_{12} = \frac{\sigma_1 + \sigma_2}{2}$$

The value of $\Omega_{12}^{(1,1)*}$ is tabulated in reference (39) for any value of KT/ε_{12}.

A summary of the calculations is presented in Table (1). It is noted that $\sigma_{12}^2\ \Omega_{12}^{(1,1)*}$ is almost constant, independent of the temperature. Substitute this value in equation (A-1), and find the following expressions for the diffusion coefficient:

Potassium - Helium

$$D_{12} = 0.348\ \frac{T^{3/2}}{p}\ ft^2/hr$$

Potassium - Argon

$$D_{12} = 0.091\ \frac{T^{3/2}}{p}\ ft^2/hr$$

where T is in ^oR and p in lb_f/ft^2.

The Thermal Conductivity of a Binary Mixture

The thermal conductivity k_m for a binary mixture is

$$k_m = \frac{1 + Z}{X + Y} = \frac{1 + Z}{X\left[1 + (Y/X)\right]}$$

where

$$X = \frac{\left(\frac{n_1}{n}\right)^2}{(k_1)} + \frac{2\left(\frac{n_1}{n}\right)\left(\frac{n_2}{n}\right)}{(k_{12})} + \frac{\left(\frac{n_2}{n}\right)^2}{k_2}$$

$$Y = \frac{\left(\frac{n_1}{n}\right)^2}{(k_1)}\, U^{(1)} + \frac{2\left(\frac{n_1}{n}\right)\left(\frac{n_2}{n}\right)}{(k_{12})}\, U^{(Y)} + \frac{\left(\frac{n_2}{n}\right)^2}{(k_2)}\, U^{(2)}$$

$$Z = \left(\frac{n_1}{n}\right)^2 U^{(1)} + 2\left(\frac{n_1}{n}\right)\left(\frac{n_2}{n}\right) U^{(2)} + \left(\frac{n_2}{n}\right)^2 U^{(2)}$$

$$U^{(1)} = \frac{4}{15} A^*_{12} - \frac{1}{12}\left(\frac{12}{5} B^*_{12} + 1\right) \frac{M_1}{M_2} + \frac{1}{2} \frac{(M_1 - M_2)^2}{M_1 M_2}$$

$$U^{(2)} = \frac{4}{15} A^*_{12} - \frac{1}{12}\left(\frac{12}{5} B^*_{12} + 1\right) \frac{M_2}{M_1} + \frac{1}{2} \frac{(M_2 - M_1)^2}{M_1 M_2}$$

$$U^{(Y)} = \frac{4}{15} A^*_{12} \left[\frac{(M_1 + M_2)^2}{4 M_1 M_2}\right] \frac{(k_{12})^2}{(k_1)(k_2)} - \frac{1}{12}\left(\frac{12}{5} B^*_{12} + 1\right)$$

$$- \frac{5}{32 A^*_{12}}\left(\frac{12}{5} B^*_{12} - 5\right) \frac{(M_1 - M_2)^2}{M_1 M_2}$$

$$U^{(X)} = \frac{4}{15} A^*_{12} \left[\left\{ \frac{(M_1 + M_2)^2}{4M_1 M_2} \right\} \left\{ \frac{(k_{12})}{(k_1)} + \frac{(k_{12})}{(k_2)} \right\} - 1 \right]$$

$$- \frac{1}{12} \left(\frac{12}{5} B^*_{12} + 1 \right)$$

where

$$(k_{12}) \times 10^7 = 1989.1 \sqrt{\frac{T(M_1 + M_2)/2 M_1 M_2}{\sigma^2_{12} \Omega_{12}^{(2,2)*}}}$$

$\frac{n_1}{n}$, $\frac{n_2}{n}$ = mole fractions of species 1 and 2

A^*_{12}, B^*_{12} = functions of $\frac{KT}{\varepsilon_{12}}$ (tabulated in reference (39))

$\Omega_{12}^{(22)}$ = collision integral

The thermal conductivities of the pure components k_1 and k_2 are obtained from the following expression

$$k \times 10^7 = \frac{1989.1 \sqrt{T/M}}{\sigma^2 \Omega^{(22)*}}$$

where k = thermal conductivity in cal/cm sec ^oK

M = molecular weight

$\Omega^{(22)}$ = collision integral

σ = parameter in potential function

The Thermal Diffusion Ratio

The thermal diffusion ratio k_T, is given approximately by the following expression

$$k_T = \frac{n_1 n_2}{6n^2 k_{12}} \frac{S^{(1)}\left(\frac{n_1}{n}\right) - S^{(2)}\left(\frac{n_2}{n}\right)}{X + Y} \quad (6\, C^*_{12} - 5)$$

where

$$S^{(1)} = \left(\frac{M_1 + M_2}{2M_2}\right) \frac{k_{12}}{k_1} - \frac{15}{4A^*_{12}} \left(\frac{M_2 - M_1}{2M_1}\right) - 1$$

$$S^{(2)} = \left(\frac{M_2 + M_1}{2M_1}\right) \frac{k_{12}}{k_2} - \frac{15}{4A^*_{12}} \left(\frac{M_1 - M_2}{2M_2}\right) - 1$$

C^*_{12} = function of $\frac{KT}{12}$ (tabulated in reference (39)).

TABLE I

SUMMARY OF POTENTIAL ENERGY PARAMETERS AND COLLISION INTEGRALS

Temperature		ε/K			$\frac{KT}{\varepsilon_{12}}$		σ			σ_{12}		$\Omega_{12}^{(11)*}$		$\Omega_{12}^{(11)*}\sigma_{12}^{2}$	
^{o}K	^{o}F	H_e	A	K	H_e-K	A - K	H_e	A	K	H_e-K	A - K	H_e-K	A - K	H_e-K	A - K
1100	1520	10.22	116	1265	9.66	2.87	2.58	3.47	4.55	3.57	4.01	0.747	0.961	9.52	15.5
1000	1340	10.22	116	1150	9.22	2.74	2.58	3.47	4.51	3.55	3.99	0.753	0.973	9.47	15.5
900	1160	10.22	116	1035	8.75	2.60	2.58	3.47	4.47	3.53	3.97	0.759	0.988	9.60	15.6
800	980	10.22	116	920	8.26	2.45	2.58	3.47	4.42	3.50	3.95	0.767	1.006	9.41	15.7
700	800	10.22	116	805	7.72	2.29	2.58	3.47	4.37	3.48	3.92	0.776	1.027	9.50	15.8
600	620	10.22	116	690	7.15	2.12	2.58	3.47	4.32	3.45	3.90	0.787	1.054	9.35	16.0

APPENDIX B

Experimental Data and Results for Saturated Potassium Vapor Condensing on a Vertical Surface

Test No.	T_v deg.F	T_w deg.F	$q_{c\ exp}$ Btu/hr.ft.	T_s deg.F	p_v Atm	p_s Atm	$\frac{(p_v-p_s)}{p_s}$	$\frac{(T_v-T_s)}{T_s}$	σ	σ emp	$q_{c\ emp}$ $\frac{Btu}{hr.ft^2}$	$h_{c\ exp}$ $\frac{Btu}{hr.ft^2\ ^oF}$	$h_{c\ emp}$ $\frac{Btu}{hr.ft^2\ ^oF}$
1	1052.50	1049.83	34403	1050.16	0.1070	0.1051	0.0185	0.0015	0.258	0.191	24579	12885	9205
2	1055.00	1050.20	53970	1050.81	0.1092	0.1056	0.0334	0.0028	0.227	0.191	44421	11243	9254
3	1132.75	1129.91	36023	1130.27	0.1947	0.1913	0.0177	0.0016	0.169	0.142	29703	12684	10458
4	1146.80	1140.91	66544	1141.74	0.2148	0.2074	0.0359	0.0032	0.145	0.136	62261	11297	10570
5	1201.50	1197.31	41074	1197.75	0.3104	0.3029	0.0247	0.0023	0.094	0.113	49861	9802	11900
6	1182.00	1179.35	42445	1179.81	0.2730	0.2690	0.0147	0.0013	0.174	0.120	28309	16017	10682
7	1233.50	1227.39	45571	1227.90	0.3807	0.3675	0.0358	0.0033	0.061	0.102	77976	7458	12762
8	1300.00	1295.85	49943	1296.44	0.5683	0.5566	0.0209	0.0020	0.077	0.083	53759	12034	12954
9	1305.00	1295.00	98824	1296.48	0.5849	0.5567	0.0506	0.0049	0.064	0.083	130459	9882	13045
10	805.50	799.00	44078	799.44	0.0106	0.0099	0.0706	0.0048	0.640	0.625	42753	6781	6577
11	811.00	800.00	80968	800.99	0.0112	0.0100	0.1186	0.0079	0.670	0.619	72093	7360	6553
12	850.73	843.50	45864	843.97	0.0172	0.0160	0.0736	0.0052	0.455	0.490	50550	6343	6991
13	914.00	902.00	80926	903.02	0.0324	0.0291	0.1110	0.0081	0.327	0.363	92031	6744	7669
14	906.50	901.30	43176	901.74	0.0301	0.0288	0.0470	0.0035	0.399	0.366	38786	8303	7458
15	1017.30	1012.00	41355	1012.42	0.0807	0.0775	0.0411	0.0033	0.193	0.223	48460	7802	9143
16*	1218.25	1216.00	29405	1216.28	0.3457	0.3414	0.0126	0.0012	0.116	0.106	26702	13069	11867

*Condensation on the lower surface of a horizontal disc. See test 11, Appendix C.

APPENDIX C

Experimental Data and Results for Potassium Condensing in the Presence of Helium

Test No.	T_1 deg F	T_o deg F	W $lb_m \times 10^{-6}$	t inches	$q_{c\ exact}$ Btu/hr.ft^2	$q_{c\ approx.}$ Btu/hr.ft^2	$q_{c\ exp}$ Btu/hr.ft^2	q_r Btu/hr.ft^2	$(q_{c\ exp}-q_r)$ Btu/hr.ft^2	$\frac{(q_{c\ exact}-q_{c\ approx.})}{q_{c\ exact}}$ per cent	$h_{c\ exact}$ Btu/hr.ft^{2}deg F	$h_{c\ approx.}$ Btu/hr.ft^{2}deg F	$h_{c\ exp}$ Btu/hr.ft^{2}deg F	$\frac{h_{c\ exp}-h_{c\ exact}}{h_{c\ exact}}$ per cent
1	1108	900	0.70	0.159	19350	19229	25000	707	24293	0.625	93.0	92.4	117.01	+ 25.8
2	1293	900	1.55	0.109	34300	33822	29500	1615	27885	1.395	87.3	85.2	71.0	- 18.7
3	1305	1129	0.70	0.050	51200	51959	42000	1045	40955	- 1.485	291.0	295.2	232.0	- 20.3
4	1312	886	2.84	0.183	20950	20462	23000	1745	21255	2.330	49.3	48.0	49.8	+ 1.0
5	1215	674	2.84	0.296	13400	12842	13000	1490	11510	4.170	24.8	23.7	21.3	- 14.1
6	1250	517	8.26	0.660	6220	5853	7000	1470	5530	5.900	8.5	8.0	7.5	- 11.8
7	1315	616	8.26	0.479	8710	8197	9700	1830	7870	5.900	12.5	11.7	11.3	- 9.6
8	1293	640	4.19	0.276	14850	14099	17000	1740	15260	5.060	22.7	21.6	23.4	+ 3.1
9	1292	630	5.78	0.381	10800	10219	15000	1725	13275	5.380	16.4	15.4	20.0	+ 21.9
10	1300	1207	0.30	0.023	71000	73100	69000	617	68383	- 2.960	764.0	786.0	735.0	- 3.8
11*	1218.25	1216.0	0.00	0.000	-	-	29405			-	-	-	13069	-

*See Appendix B

APPENDIX D

Experimental Data and Results for Potassium Condensing in the Presence of Argon

Test No.	T_1 deg F	$T_{o\ min}$ deg F	$T_{o\ max}$ deg F	W $lb_m \times 10^{-6}$	t inches	$q_{c\ exact}$ Btu/hr.ft^2	$q_{c\ approx.}$ Btu/hr.ft^2	$q_{c\ exp}$ Btu/hr.ft^2	q_r Btu/hr.ft^2	$(q_{c\ exp}-q_r)$ Btu/hr.ft^2	$\frac{(q_{c\ exact}-q_{c\ approx.})}{q_{c\ exact}}$ per cent	$h_{c\ exact}$ Btu/hr.ft^{2}deg F	$h_{c\ approx.}$ Btu/hr.ft^{2}deg F	$h_{c\ exp}$ Btu/hr.ft^{2}deg F	$\frac{h_{c\ exp}-h_{c\ exact}}{h_{c\ exact}}$ per cent
1	1235	1005	1027	8.82	0.091	8750	8834	18000	1055	16945	- 0.96	38.00	38.41	73.8	+ 94.2
2	1304	1062	1095	8.81	0.063	12700	12919	23500	1295	22205	- 1.73	52.50	53.38	91.8	+ 75.0
3	1379	1170	1187	8.56	0.042	16740	17196	27500	1400	26100	- 2.73	80.00	82.28	124.8	+ 55.0
4	1407	1085	1118	23.87	0.101	8850	8900	25500	1970	23530	- 0.57	27.50	27.64	73.1	+ 166.0
5	1325	819	832	61.14	0.359	2850	2796	7000	1890	5110	1.90	5.63	5.52	10.2	+ 81.1
6	1365	766	770	106.93	0.263	2100	2047	6100	2140	3960	2.52	3.51	3.42	6.6	+ 88.1
7	1291	920	1005	9.88	0.072	13000	13136	29200	1575	27625	- 1.05	35.0	35.41	74.5	+ 113.0
8	1378	870	1030	14.72	0.067	15000	15110	29200	2170	27030	- 0.73	29.50	29.74	53.3	+ 80.7
9	1413	898	910	18.69	0.072	14000	14071	29000	2430	26570	- 0.51	27.20	27.32	51.7	+ 90.0
10	1414	773	795	31.72	0.117	9000	8878	23000	2430	20570	0.24	14.05	13.85	32.1	+ 128.5
11	1398	718	733	33.83	0.133	8000	7850	19800	2360	17440	1.88	11.77	11.54	25.7	+ 118.5
12	1412	1300	1303	6.09	0.027	17000	17541	30000	1035	28965	- 3.18	152.00	156.62	259.0	+ 70.4
13	1350	1200	1205	5.26	0.031	19000	19655	32000	1025	30975	- 3.45	126.60	131.04	206.0	+ 62.7
14	1300	1250	1252	1.28	0.010	25000	26248	39600	353	39247	- 5.00	500.00	524.00	784.9	+ 56.8

-57-

APPENDIX E

Temperature Profile in the Potassium Vapor

Consider the system as shown in Figure 1 where pure saturated vapor at temperature T_v condenses on a surface at temperature T_w. Previous investigators have always assumed the temperature in the vapor to be uniform in their solution of the Hertz-Knudsen equation. Although this assumption is reasonable in many cases, it is not rigorous as was shown by Bornhorst[22] recently.

Applying the energy equation to the vapor, neglecting viscous dissipation, yields

$$\frac{dT}{dx} = \frac{k}{wc_p} \frac{d^2T}{dx^2} \tag{E-1}$$

Integrate (E-1) with $T(\infty) = T_v$ and $T(0) = T_i$ to give

$$T - T_v = (T_i - T_v) \exp^{\frac{xwc_p}{k}} \tag{E-2}$$

Differentiate (E-2) and find

$$\left(\frac{dT}{dx}\right)_{x=0} = - \frac{wc_p}{k} (T_v - T_i) \tag{E-3}$$

A further expression for $\left(\frac{dT}{dx}\right)_{x=0}$ may be obtained by considering the energy flux in the vapor at the interface; i.e.,

$$J_u = h_i w - k\left(\frac{dT}{dx}\right)_{x=0} \tag{E-4}$$

According to Bornhorst[22] this same energy flux may be expressed in the following form:

$$J_u = \left(\frac{w}{K_b + 1}\right)(K_b\, h_l + h_i) - \frac{L_k(T_i - T_s)}{T_s^2} \qquad \text{(E-5)}$$

Equating (E-4) to (E-5) gives

$$\left(\frac{dT}{dx}\right)_{x=0} = \frac{K_b}{(K_b + 1)}\,\frac{h_{fg} w}{k} + \frac{L_k(T_i - T_s)}{k\, T_s^2} \qquad \text{(E-6)}$$

where

$$\frac{K_b}{(K_b + 1)} = \frac{p_s\, v_{fg}}{2\, h_{fg}}$$

and

$$L_k = \left(\frac{MT_s}{2\pi R}\right)^{1/2} (\gamma + 1)\, c_v\, p_s\, T_s$$

The following expression for $(T_i - T_v)$ is obtained by equating equation (E-3) to (E-6) and employing equation (33) for the mass flux.

$$T_i - T_v = \frac{p v_{fg}}{2\, c_p} + \frac{(\gamma + 1)(2 - \sigma)\, T_s}{2\,\gamma\sigma\left[0.5 - \frac{T_s(p_v - p_s)}{p_s(T_i - T_s)}\right]}$$

Figures

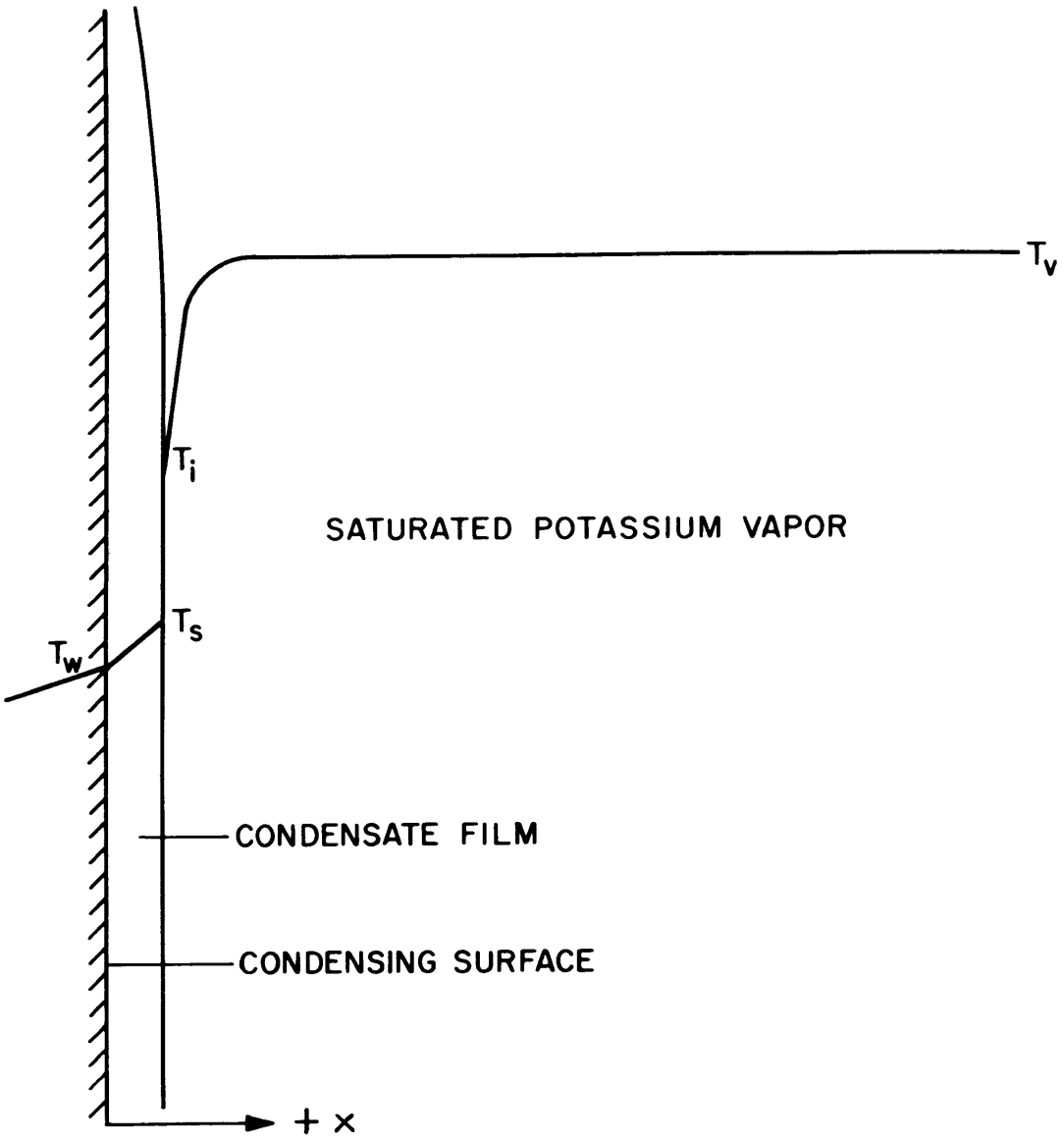

FIGURE 1 FILM CONDENSATION OF POTASSIUM VAPOR

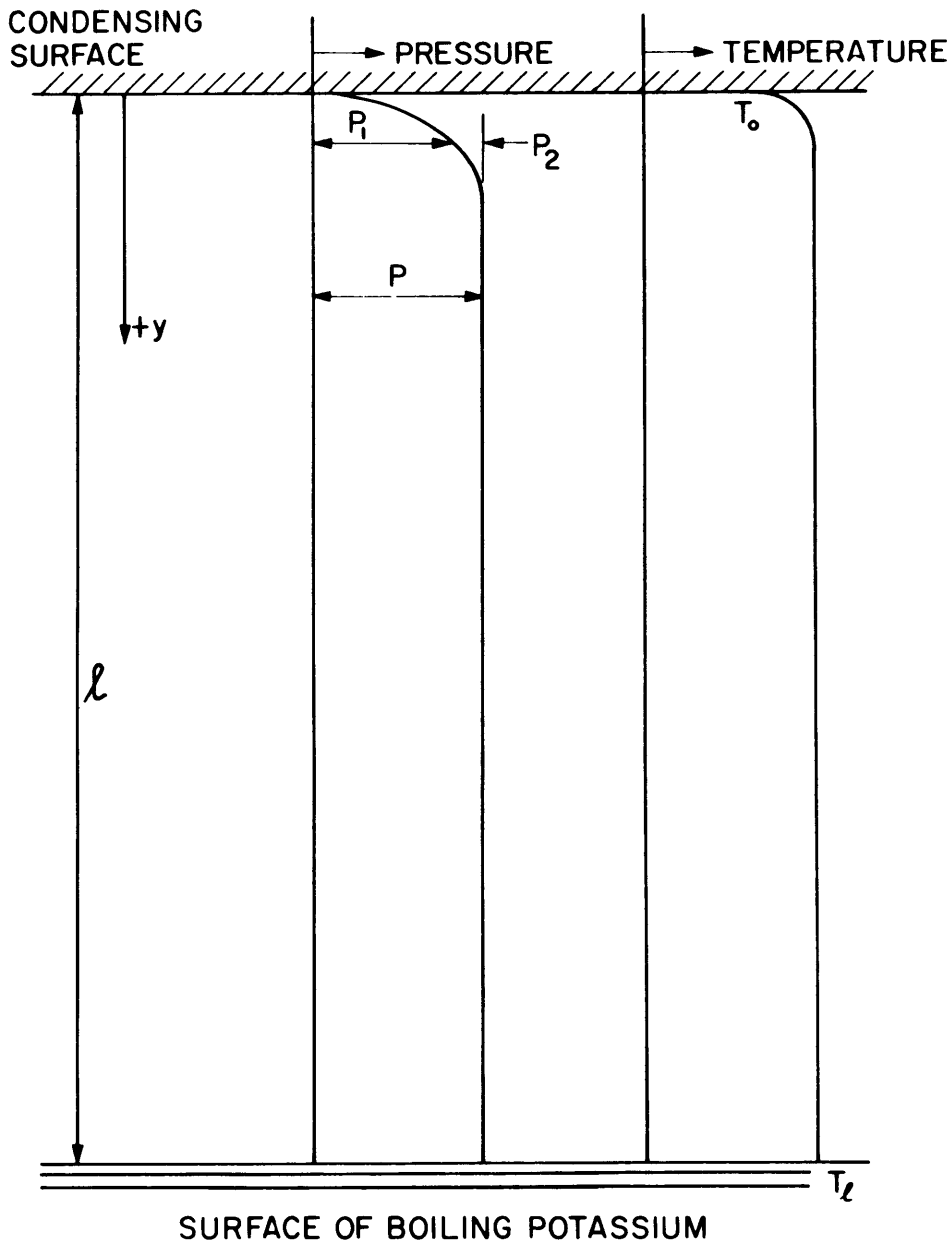

FIGURE 2 CONDENSATION OF POTASSIUM VAPOR IN THE PRESENCE OF A NON-CONDENSABLE GAS

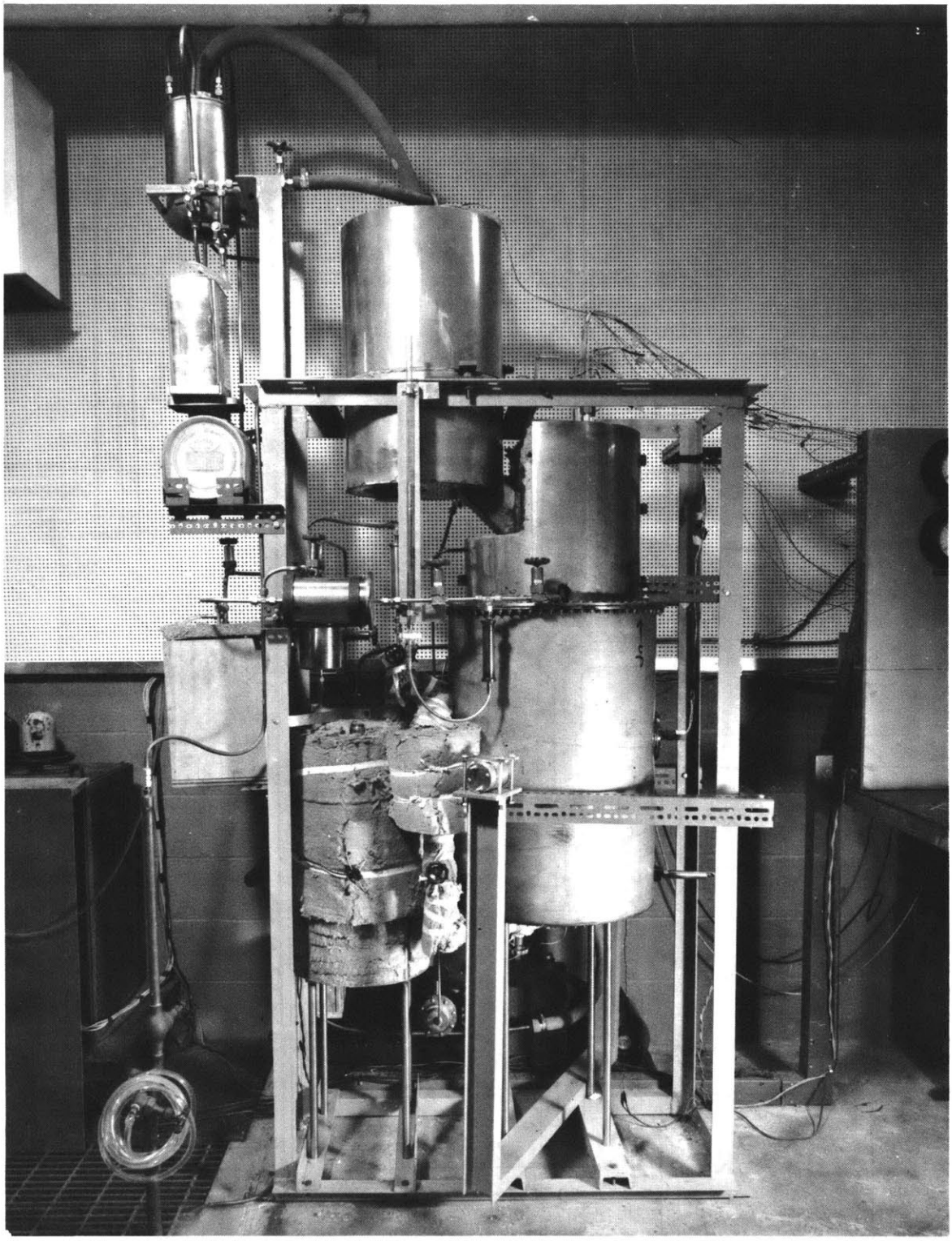

FIGURE 3. APPARATUS

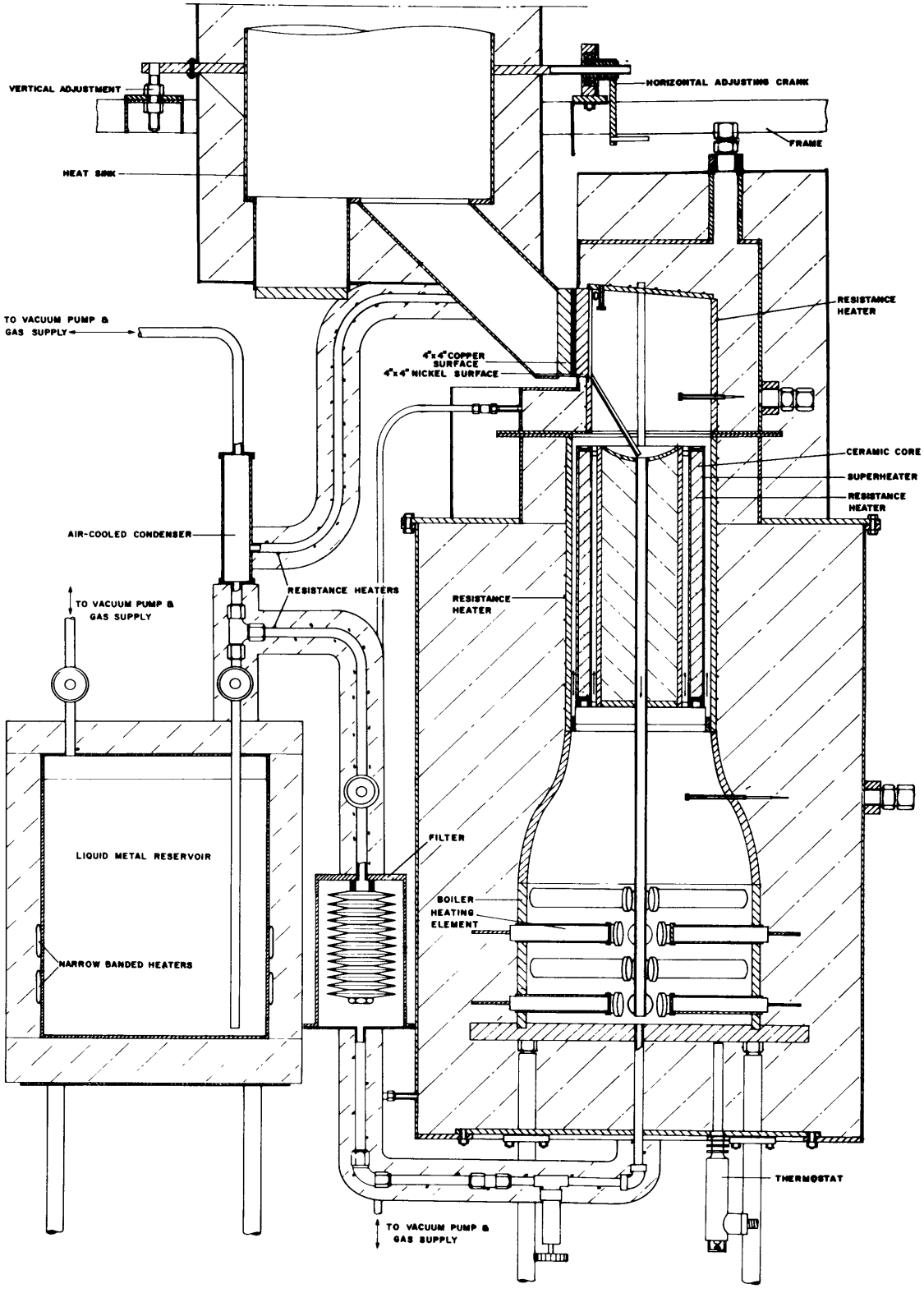

FIGURE 4 APPARATUS

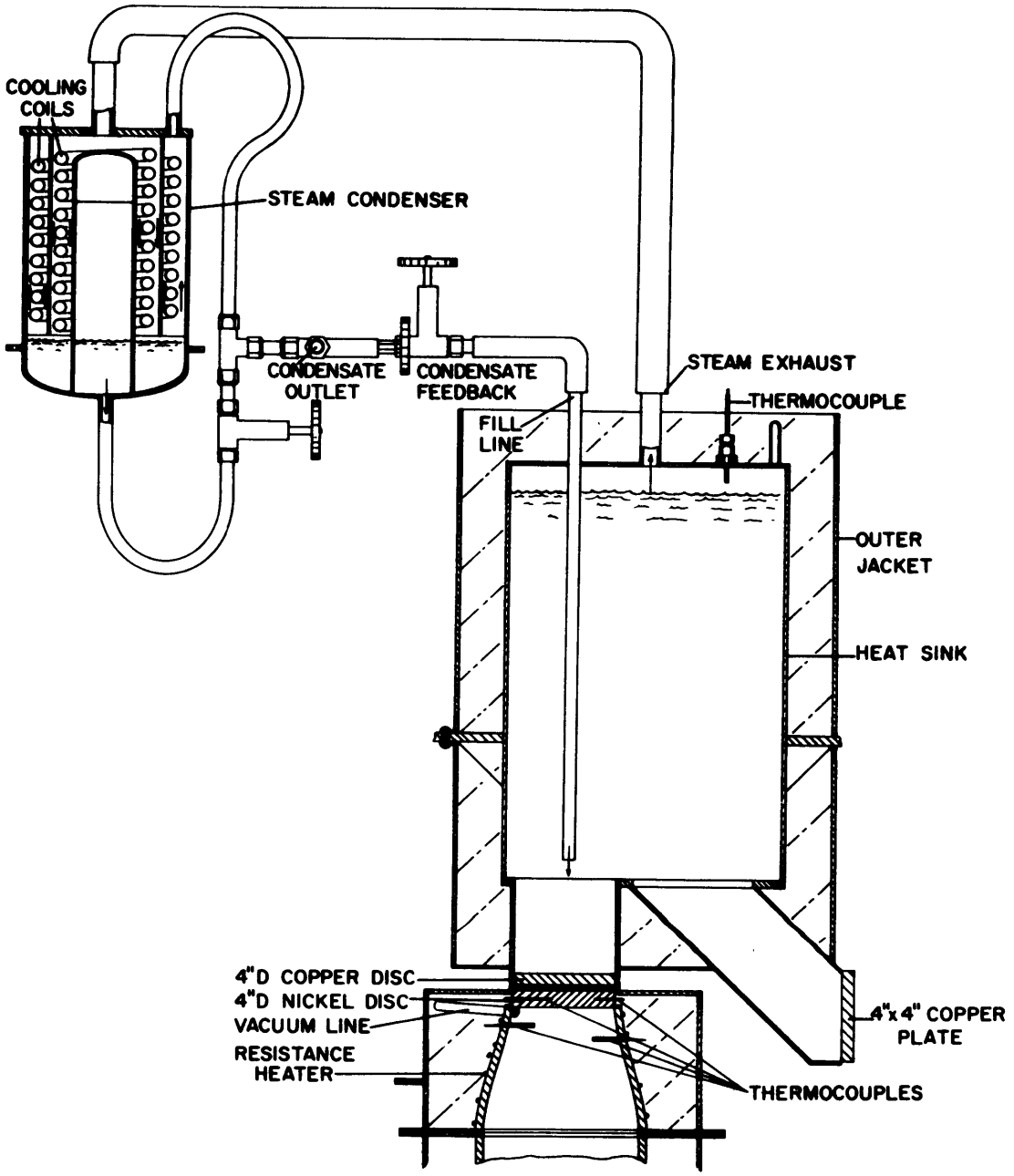

FIGURE 5 CONSTANT TEMPERATURE HEAT SINK LOCATED ABOVE THE HORIZONTAL CONDENSING SURFACE

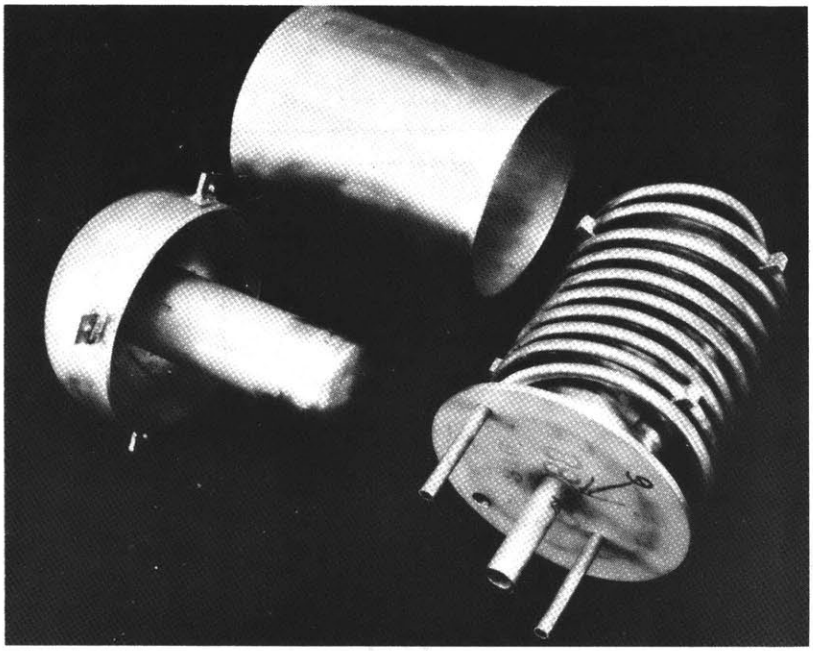

FIGURE 6. COMPONENTS OF WATER-COOLED CONDENSER

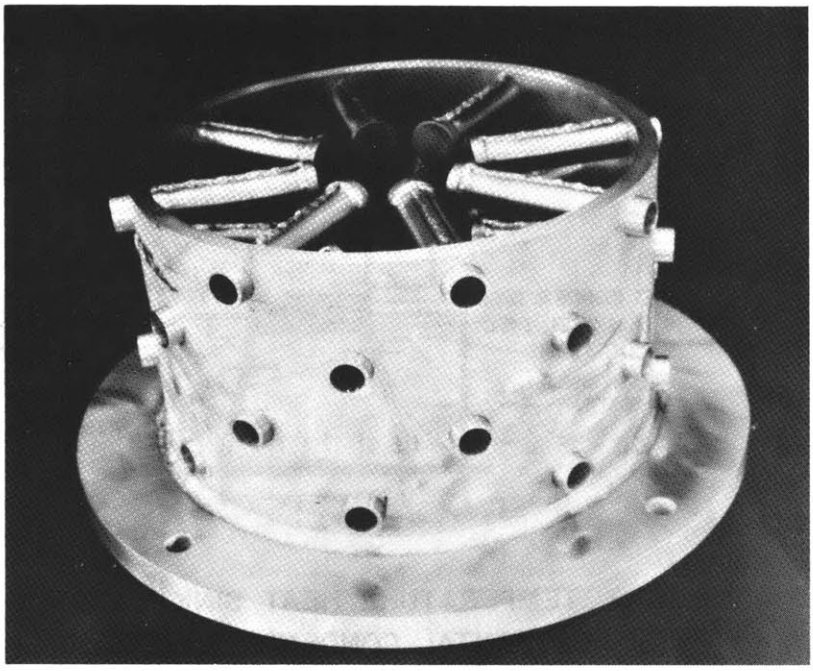

FIGURE 7. BOILER SECTION

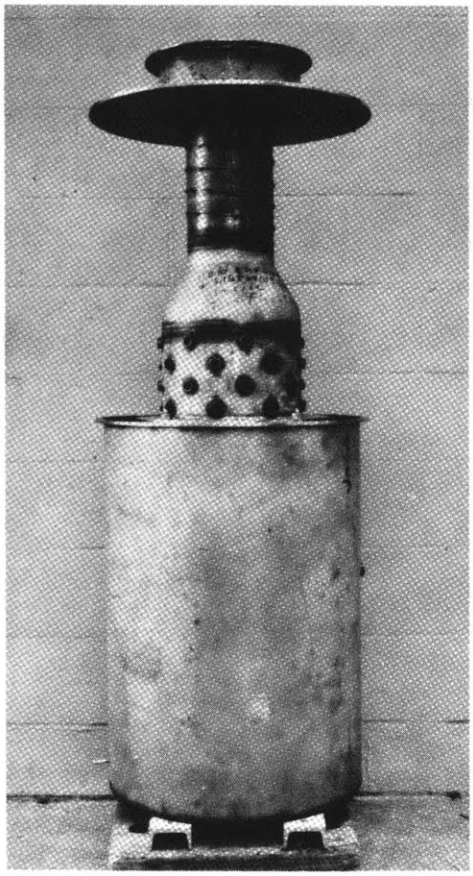

FIGURE 8. BOILER, SUPERHEATER AND JACKET

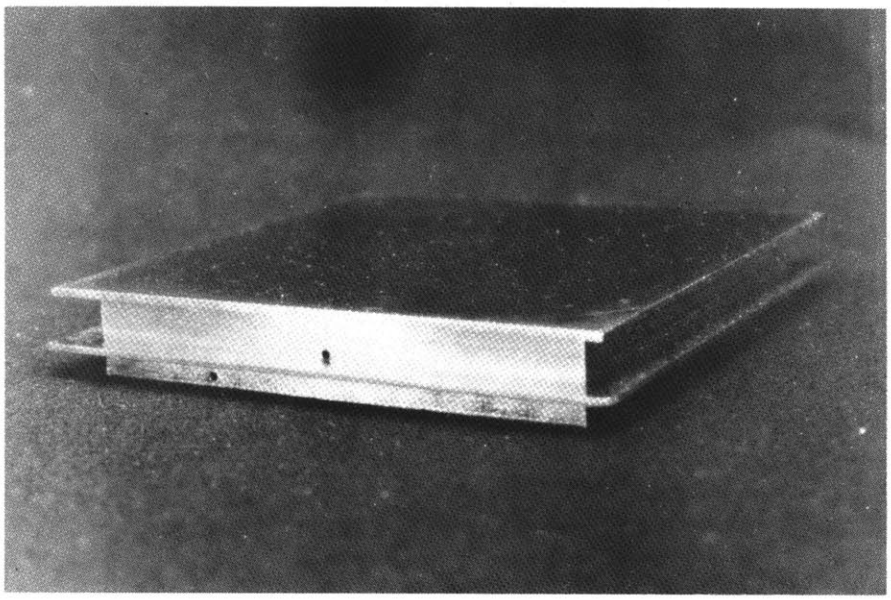

FIGURE 9. SQUARE CONDENSING SURFACE

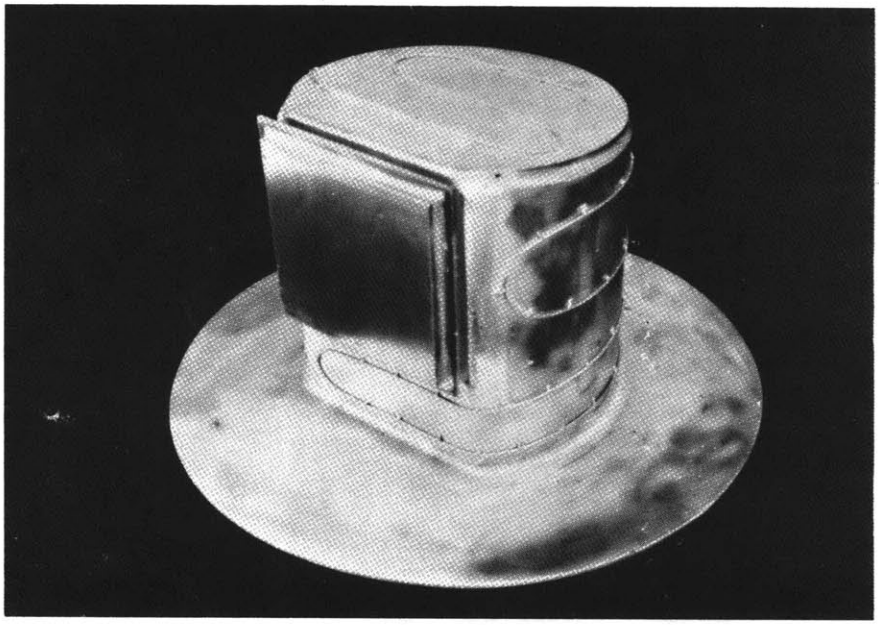

FIGURE 10. COMPLETE CONDENSING UNIT WITH VERTICAL SQUARE SURFACE

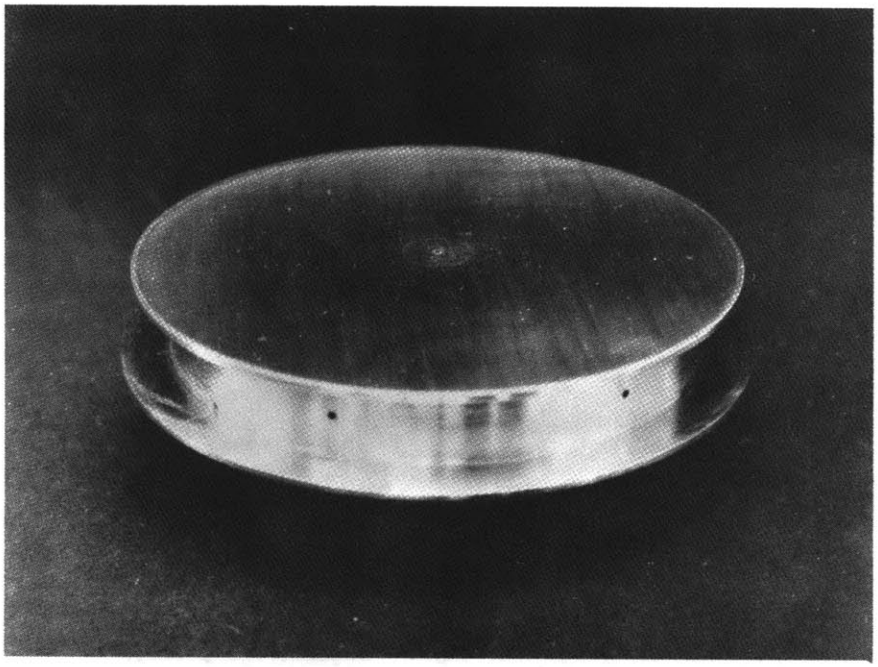

FIGURE 11. ROUND CONDENSING SURFACE

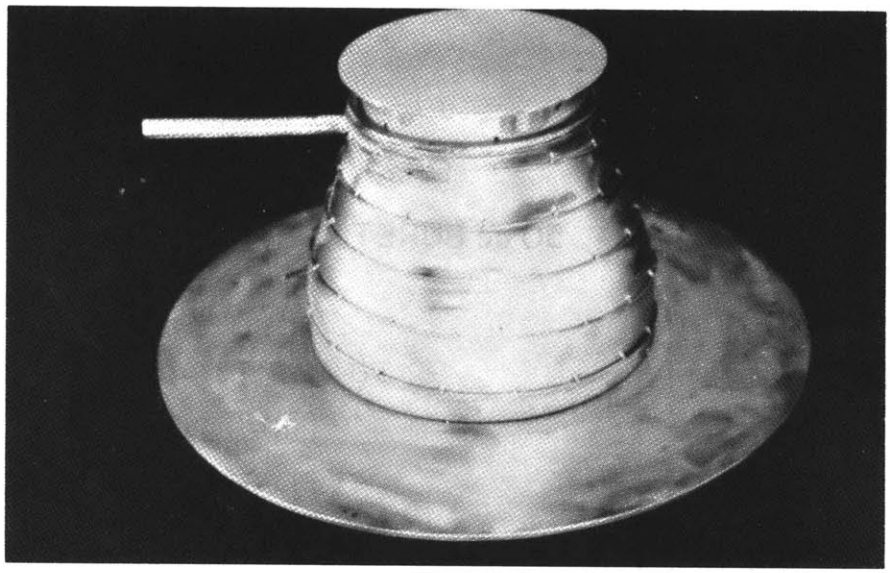

FIGURE 12. COMPLETE CONDENSING UNIT WITH ROUND HORIZONTAL SURFACE

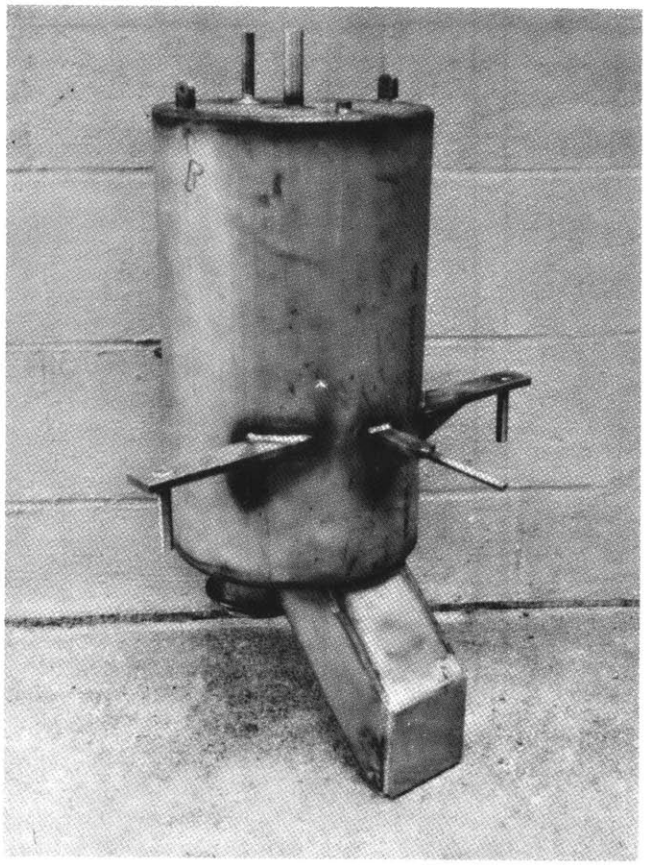

FIGURE 13. HEAT SINK

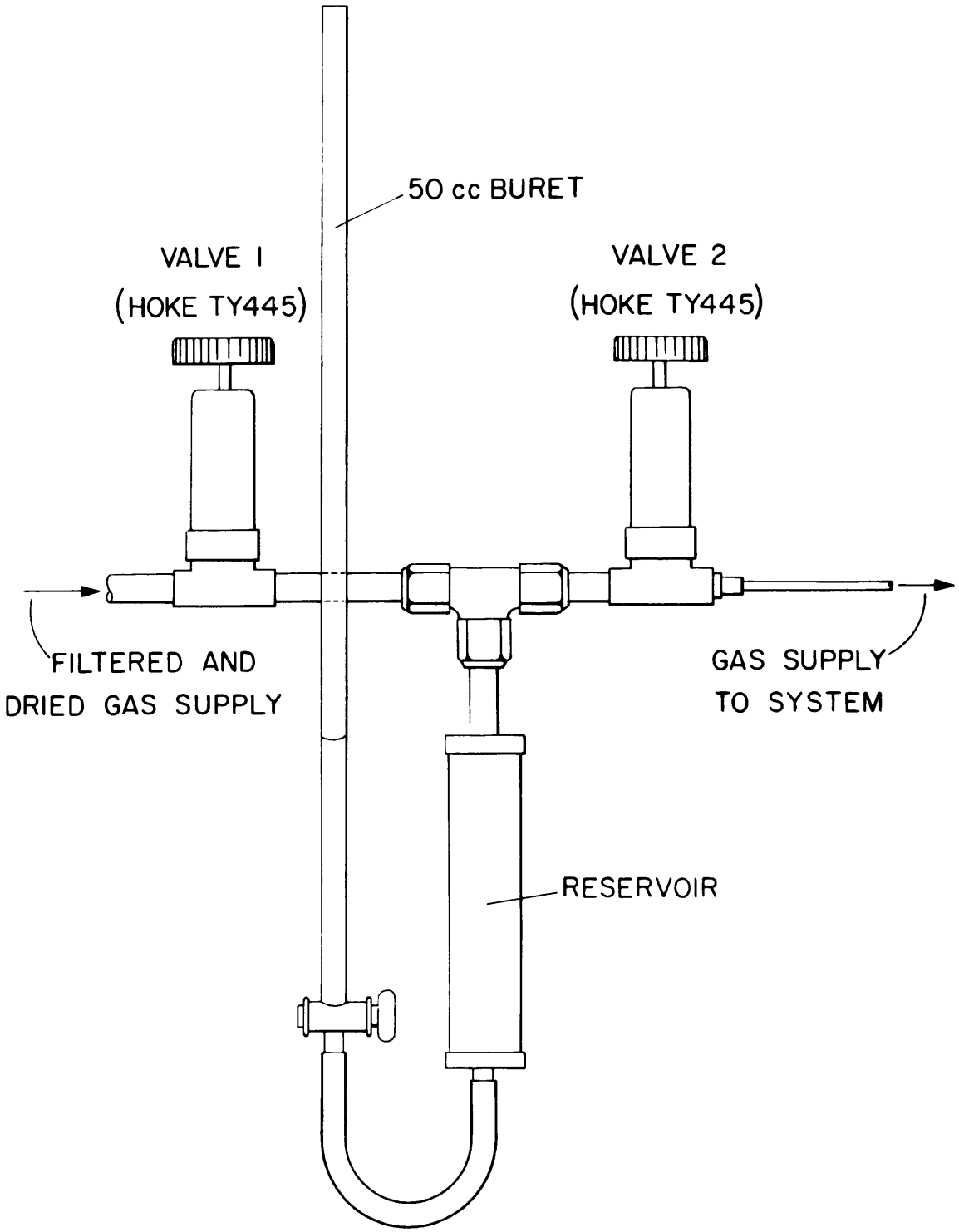

FIGURE 14 INTRODUCTION OF NON-CONDENSABLES

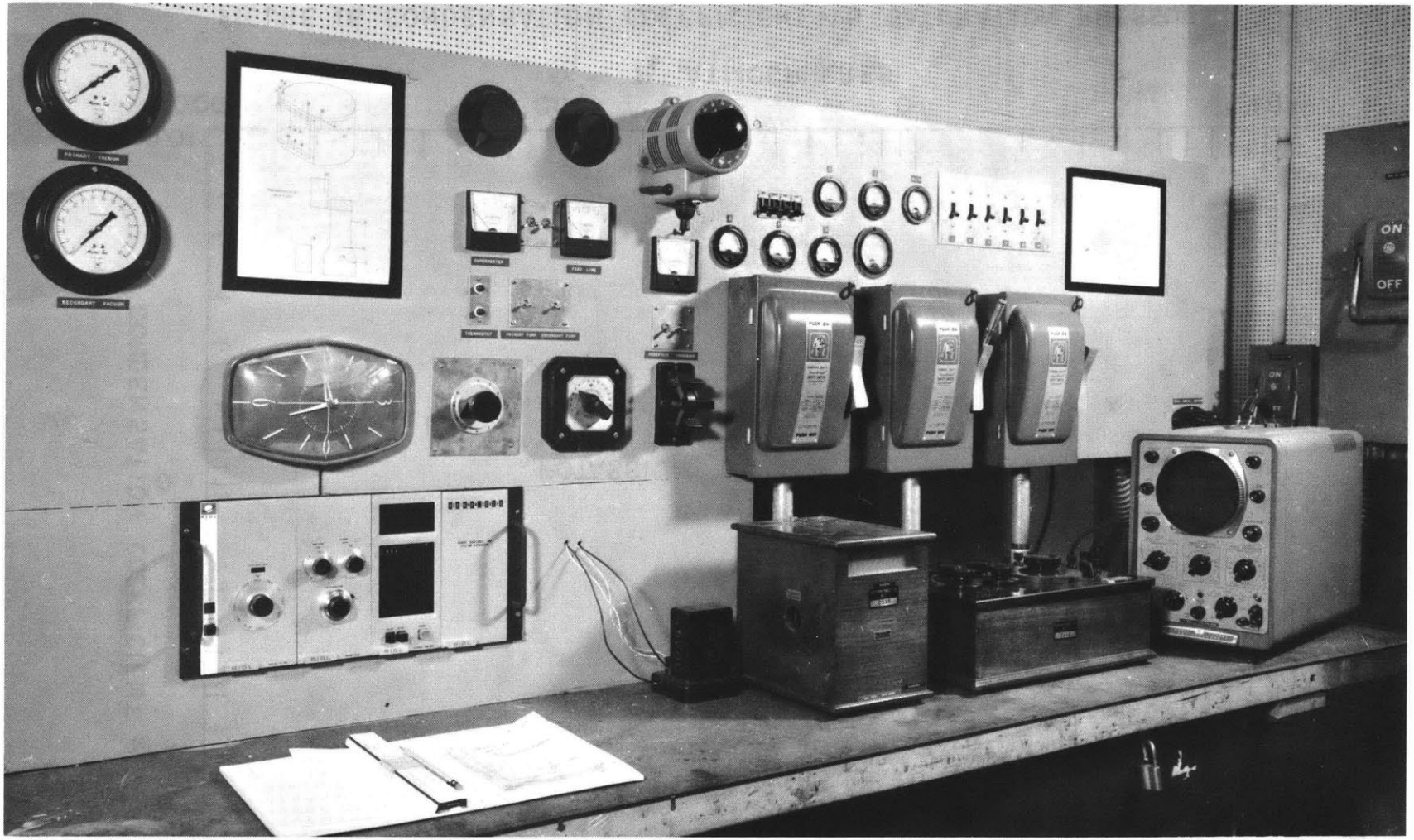

FIGURE 15. CONTROL PANEL

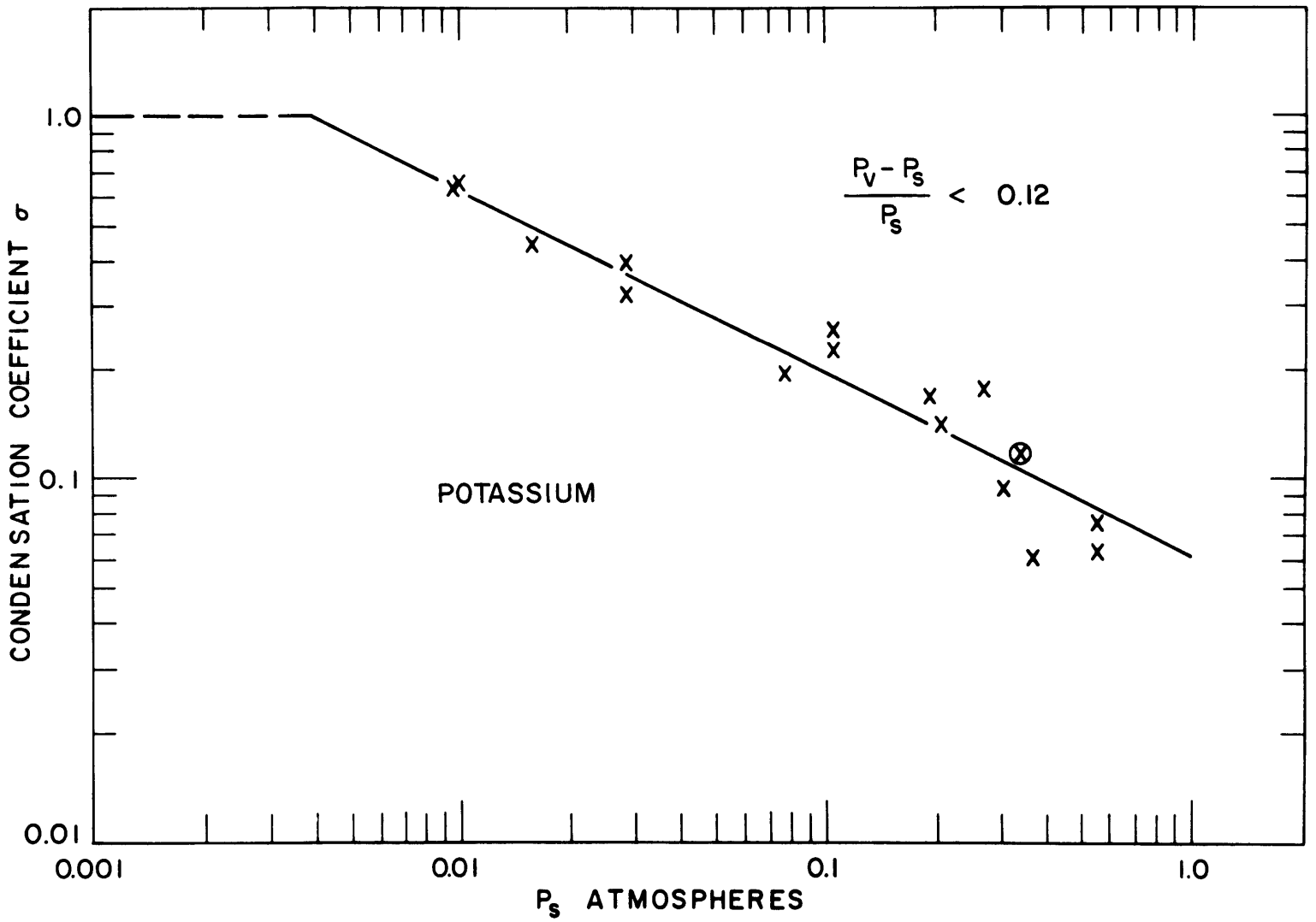

FIGURE 16 CONDENSATION COEFFICIENT VS. SATURATION PRESSURE

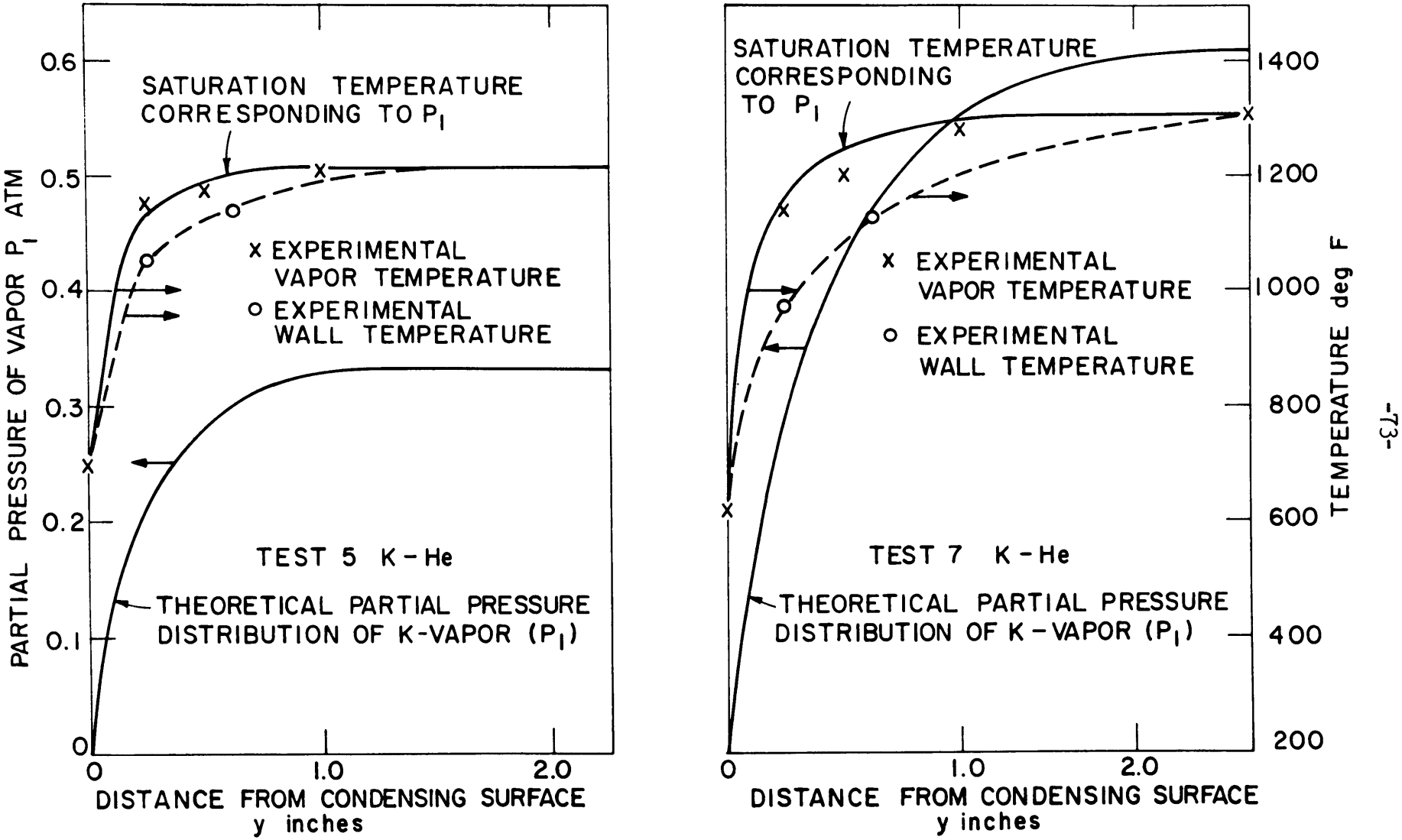

FIGURE 17 PARTIAL PRESSURE AND TEMPERATURE DISTRIBUTION VS. DISTANCE FROM CONDENSING SURFACE

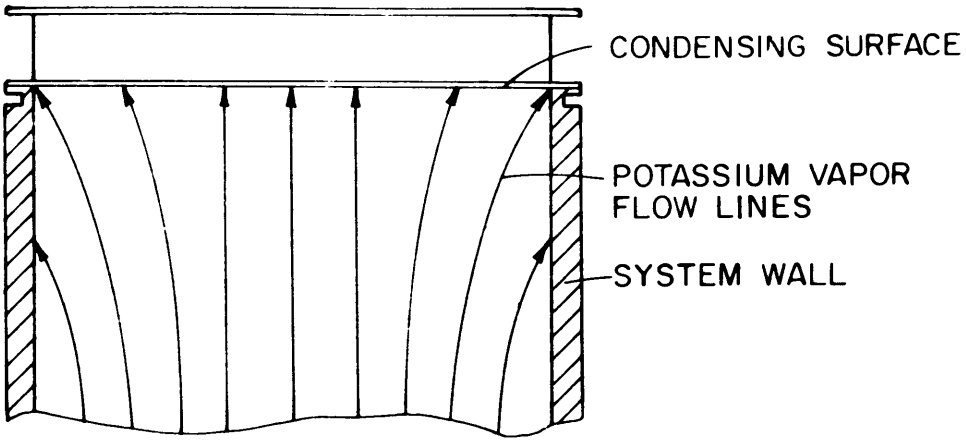

FIGURE 18 DIFFUSION FLOW FIELD IN THE PRESENCE OF A CONSIDERABLE QUANTITY OF NON-CONDENSABLE GAS

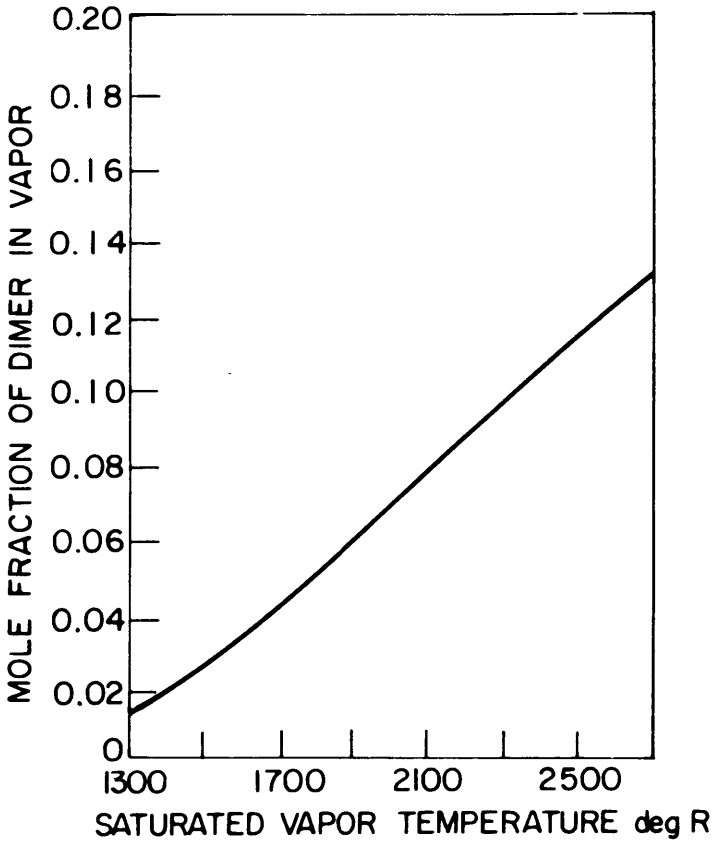

FIGURE 19 DIMERIC COMPOSITION OF POTASSIUM VAPOR

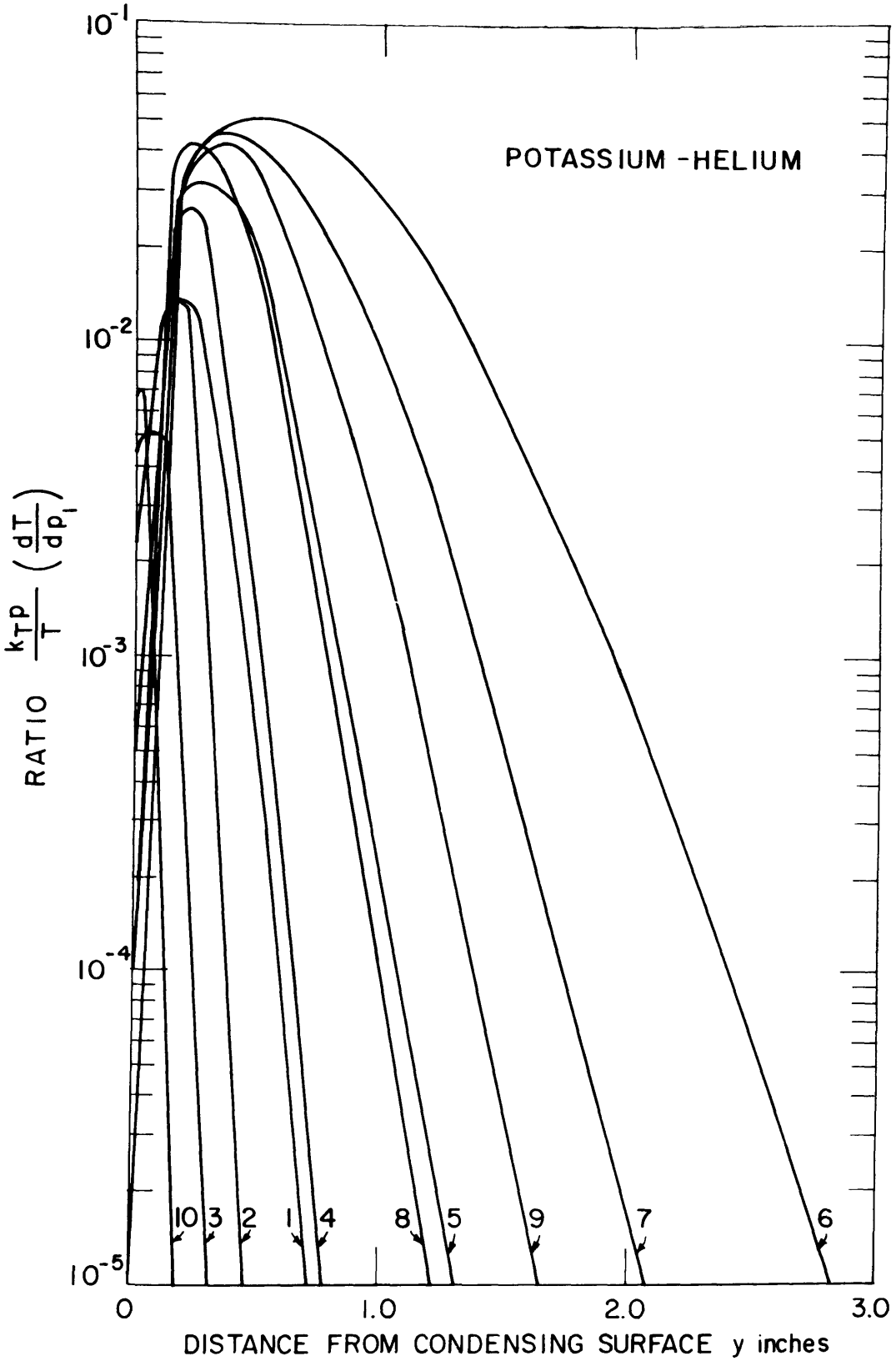

FIGURE 20 RATIO $\frac{k_T p}{T}\left(\frac{dT}{dp_1}\right)$ VS. DISTANCE FROM CONDENSING SURFACE FOR DIFFERENT TESTS

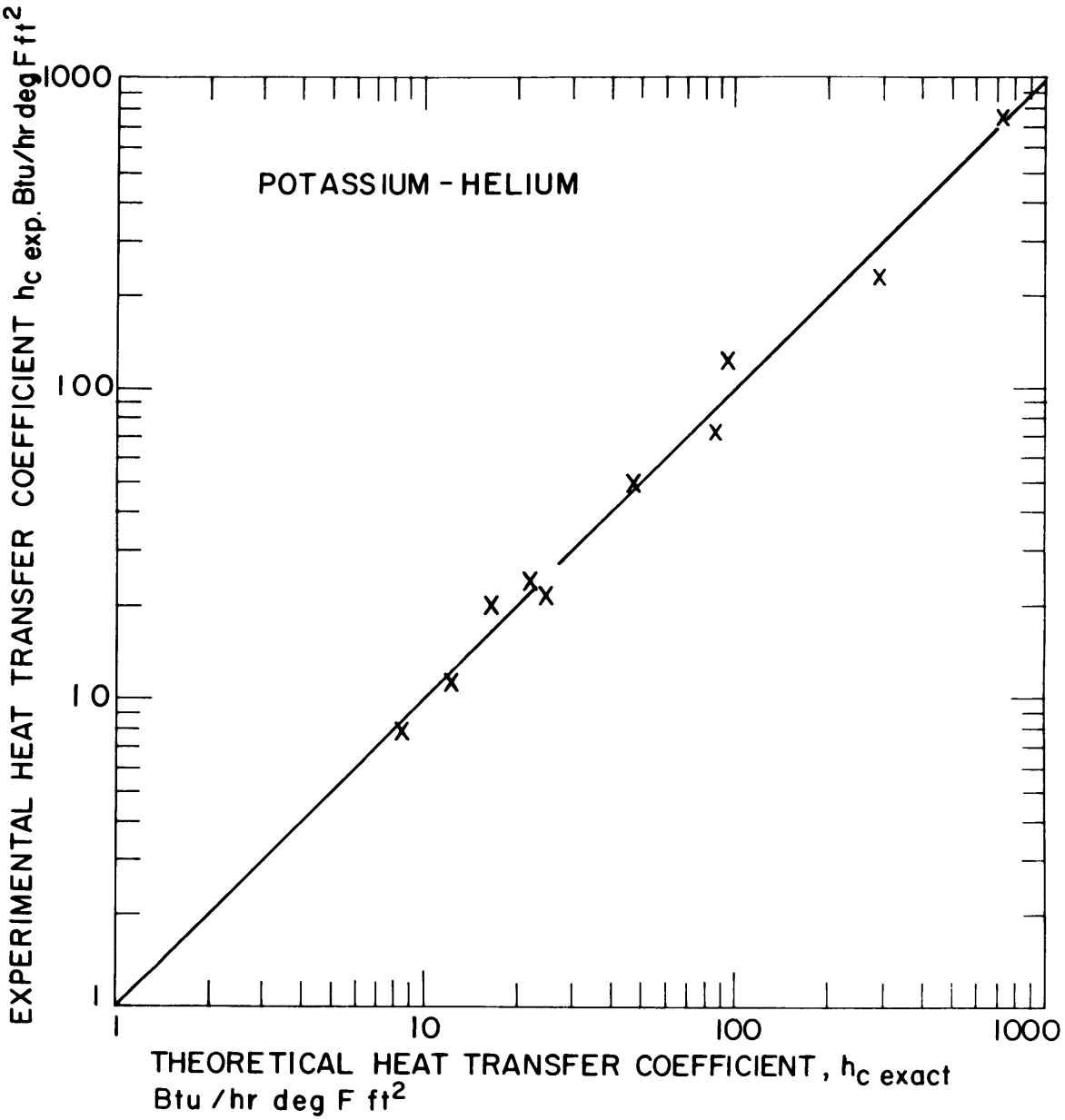

FIGURE 21 COMPARISON OF EXPERIMENTAL HEAT TRANSFER COEFFICIENT TO THEORETICAL HEAT TRANSFER COEFFICIENT

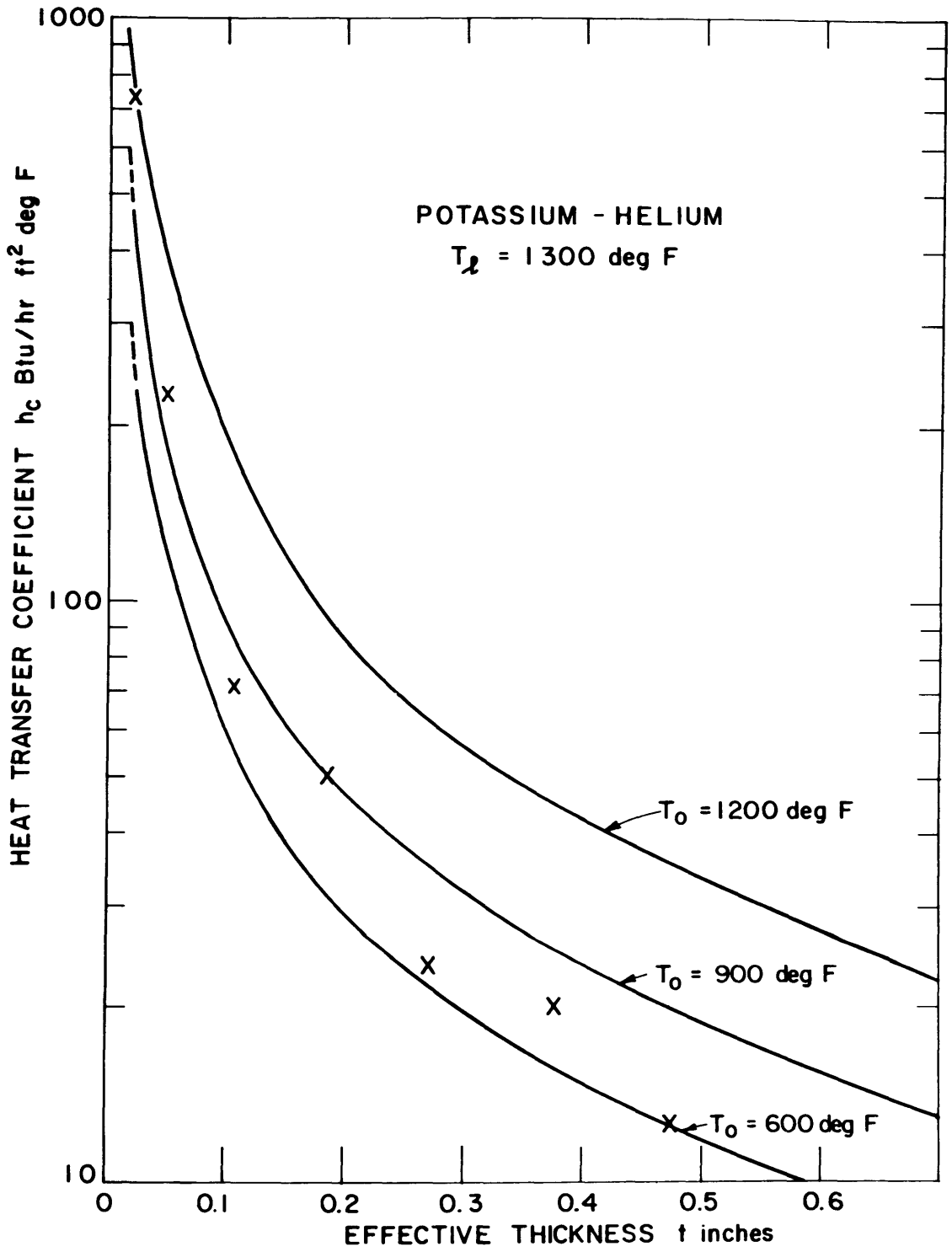

FIGURE 22 HEAT TRANSFER COEFFICIENT VS. EFFECTIVE GAS THICKNESS

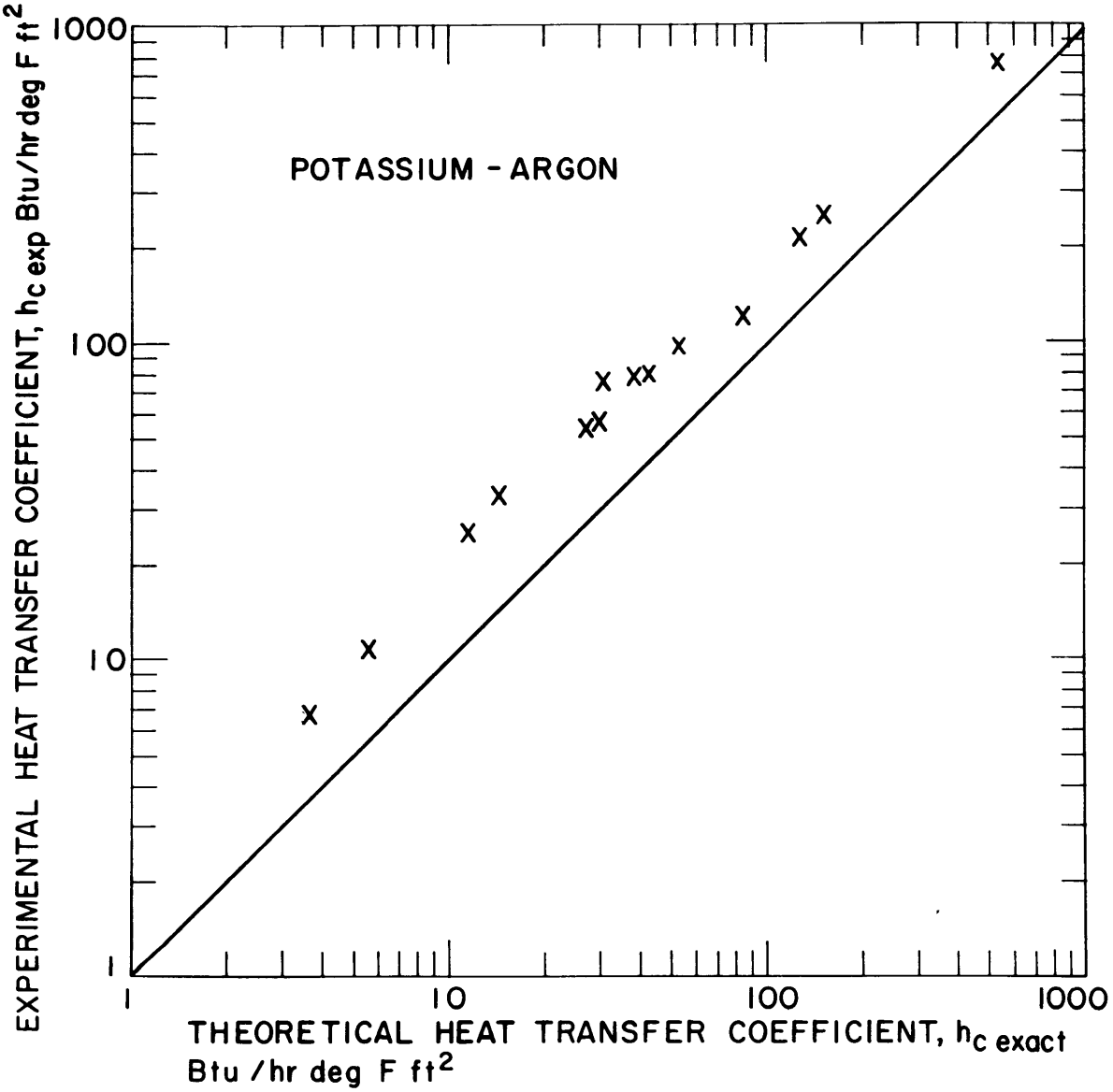

FIGURE 23 COMPARISON OF EXPERIMENTAL HEAT TRANSFER COEFFICIENT TO THEORETICAL HEAT TRANSFER COEFFICIENT

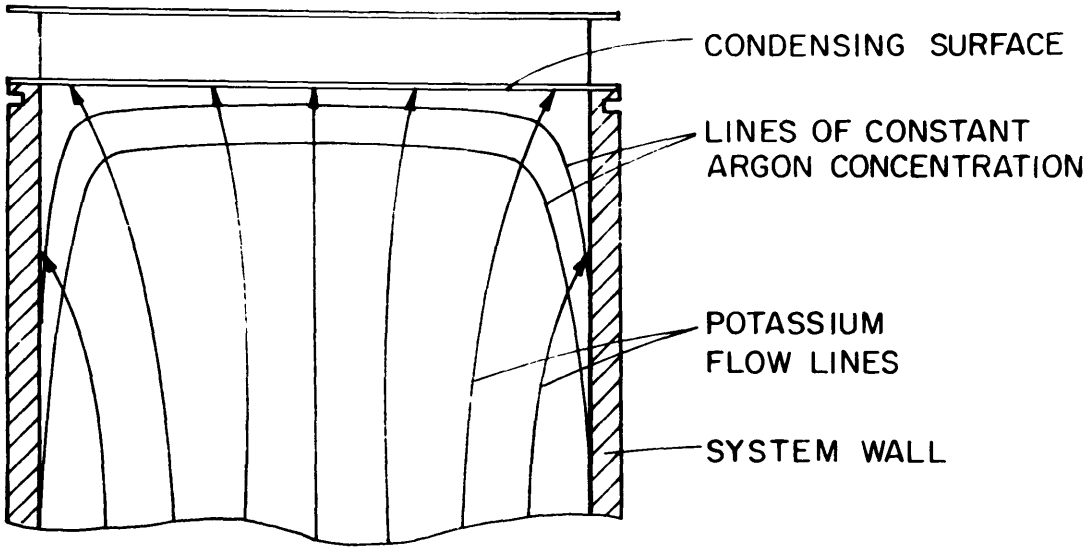

FIGURE 24 POTASSIUM CONDENSING IN THE PRESENCE OF ARGON

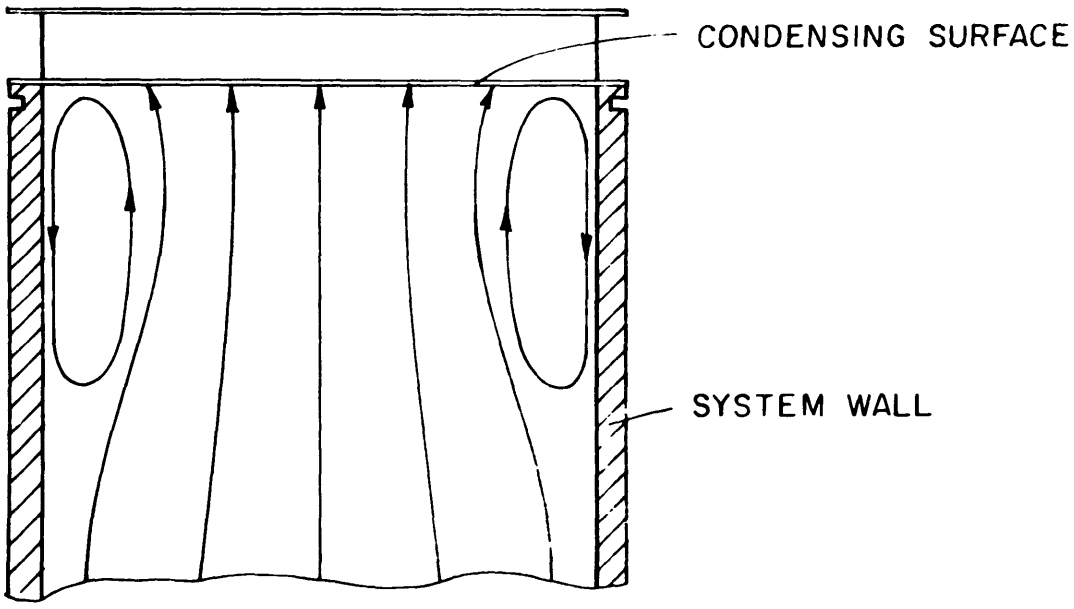

FIGURE 25 CONVECTIVE PATTERN DUE TO DENSITY GRADIENTS AT THE WALL

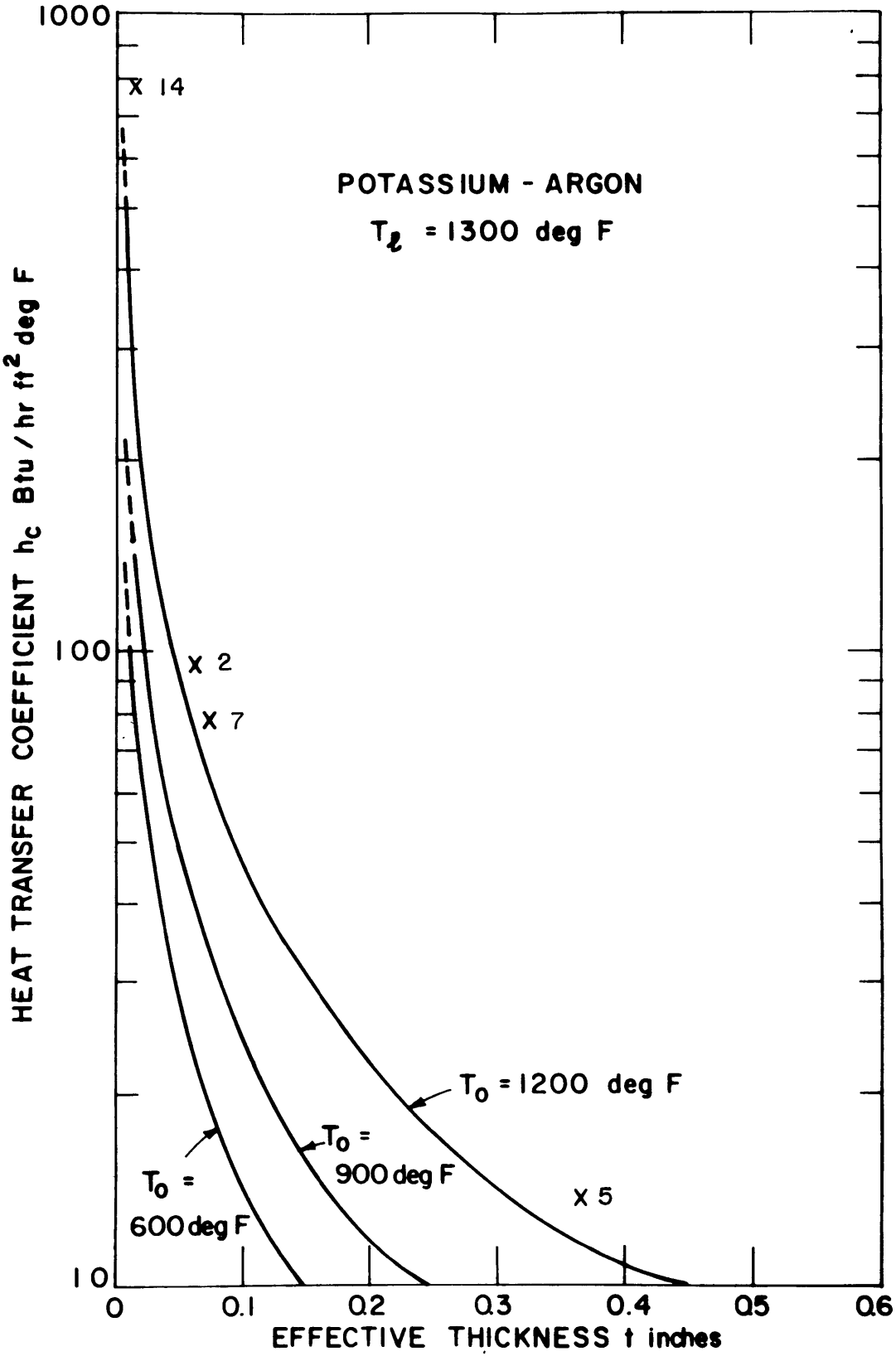

FIGURE 26 HEAT TRANSFER COEFFICIENT VS. EFFECTIVE THICKNESS

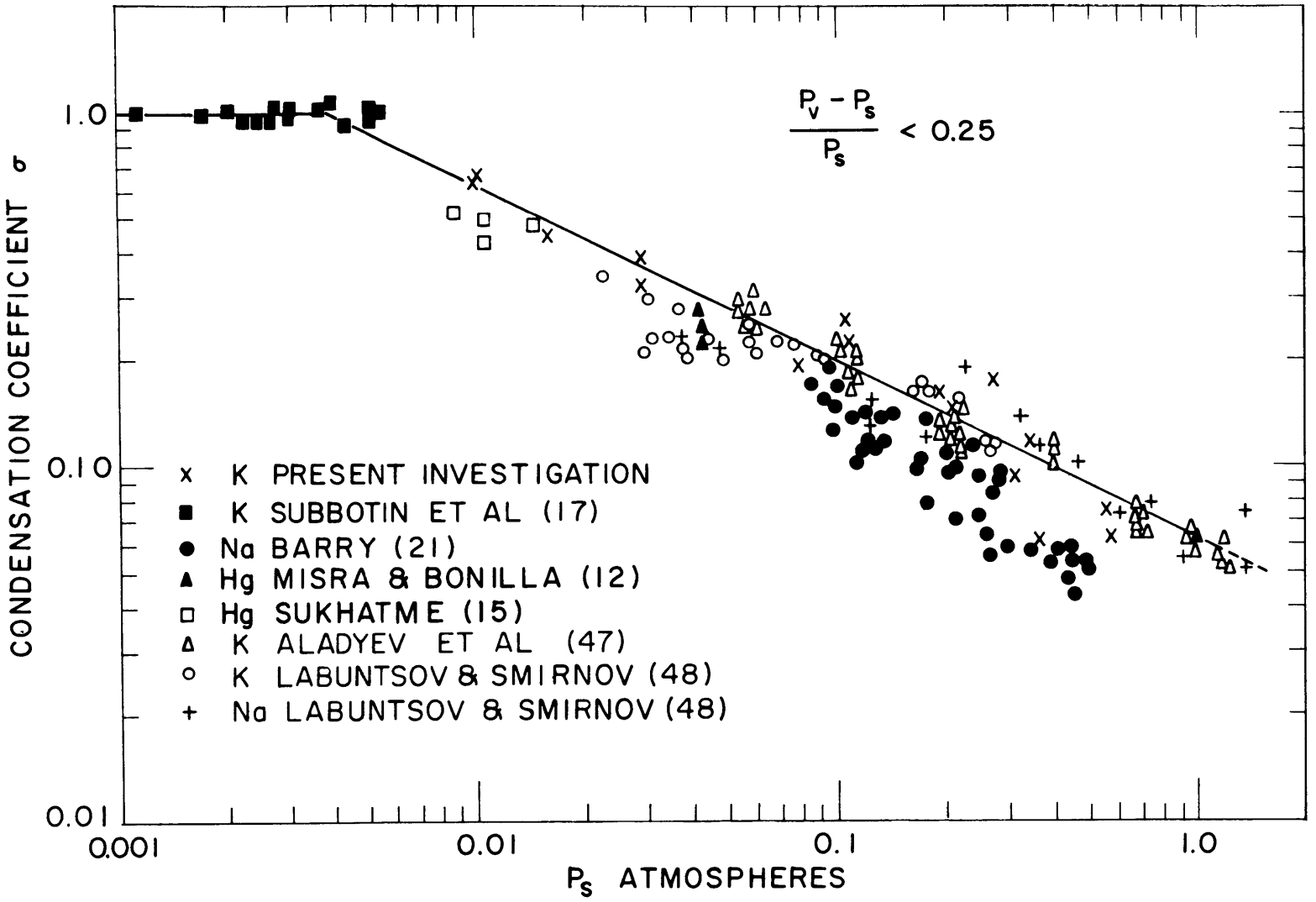

FIGURE 27 CONDENSATION COEFFICIENT VS SATURATION PRESSURE